NASA/TM—2001-211134

Specimens and Reusable Fixturing for Testing Advanced Aeropropulsion Materials Under In-Plane Biaxial Loading

Part 1—Results of Conceptual Design Study

J.R. Ellis
Glenn Research Center, Cleveland, Ohio

G.S. Sandlass
MTS Systems Corporation, Eden Prairie, Minnesota

M. Bayyari
Research Applications, Inc., San Diego, California

National Aeronautics and
Space Administration

Glenn Research Center

October 2001

Available from

NASA Center for Aerospace Information
7121 Standard Drive
Hanover, MD 21076

National Technical Information Service
5285 Port Royal Road
Springfield, VA 22100

Available electronically at http://gltrs.grc.nasa.gov/GLTRS

SPECIMENS AND REUSABLE FIXTURING FOR TESTING ADVANCED AEROPROPULSION MATERIALS UNDER IN-PLANE BIAXIAL LOADING

PART 1—RESULTS OF CONCEPTUAL DESIGN STUDY

J. R. Ellis*
National Aeronautics and Space Administration
Glenn Research Center
Cleveland, Ohio 44135

G.S. Sandlass†
MTS Systems Corporation
Eden Prairie, Minnesota 55344

M. Bayyari‡
Research Applications, Inc.
San Diego, California 92121

SUMMARY

A design study was undertaken to investigate the feasibility of using simple specimen designs and reusable fixturing for in-plane biaxial tests planned for advanced aeropropulsion materials. Materials of interest in this work include: advanced metallics, polymeric matrix composites, metal and intermetallic matrix composites, and ceramic matrix composites. Early experience with advanced metallics showed that the cruciform specimen design typically used in this type of testing was impractical for these materials, primarily because of concerns regarding complexity and cost. The objective of this research was to develop specimen designs, fixturing, and procedures which would allow in-plane biaxial tests to be conducted on a wide range of aeropropulsion materials while at the same time keeping costs within acceptable limits. With this goal in mind, a conceptual design was developed centered on a specimen incorporating a relatively simple arrangement of slots and fingers for attachment and loading purposes. The ANSYS finite element code was used to demonstrate the feasibility of the approach and also to develop a number of optimized specimen designs. The same computer code was used to develop the reusable fixturing needed to position and grip the specimens in the load frame. The design adopted uses an assembly of slotted fingers which can be reconfigured as necessary to obtain optimum biaxial stress states in the specimen gage area. Most recently, prototype fixturing was manufactured and is being evaluated over a range of uniaxial and biaxial loading conditions.

INTRODUCTION

One technique for investigating material behavior under complex stress states is to use in-plane biaxial loading. Using this approach, cruciform specimens fabricated from plate or sheet material are gripped at four locations and loaded along two orthogonal axes. Servohydraulic loading systems are used in this application which are similar to those used for uniaxial testing. Thus, the technique has the advantage that the loading arrangement is relatively straightforward and uses equipment which has seen

*Senior Research Engineer.
†Structural Analyst.
‡Principal Research Engineer.

extensive development over the past 30 years. Also, the test method allows a wide range of biaxial stress states to be investigated with minimum complication from the load application viewpoint. For these reasons, the test method has been used to generate a sizable body of biaxial test data for both monolithic and composite materials (refs. 1 to 29).

One difficulty facing these investigations has been the selection and/or development of the most suitable specimen design for the particular program. It should be noted that consensus standards do not exist for this method of testing, and so the experimentalist is faced with a wide range of possibilities. A major complication here is that use of the cruciform specimen configuration and associated gripping fixtures results in "coupling" between the two loading directions. In the present research, specimens are positioned in the load frame using four hydraulic grips which rigidly constrain the specimen over the gripped regions. It follows that loading applied in one direction is partially reacted by the specimen and partially by the grips associated with loading in the second direction. One method of minimizing this effect is to use specimen designs which incorporate fairly complicated arrangements of flexures as illustrated in figure 1. It has been demonstrated that flexures with low bending stiffness in the plane of loading can be used to minimize the constraint imposed by specimen gripping. Also, it has been shown that the geometry of the flexures can be optimized and tailored to give near-uniform stress/strain conditions in the gage area for specific biaxial loading conditions.

One obvious disadvantage of using flexures is that regions of high stress concentration can be introduced into specimens in close proximity to the gage area. Of particular concern are stress concentrations at the ends and intersection points of the flexures. This raises the possibility that failure can be initiated outside of the gage area in regions where stress/strain conditions are ill defined. Traditionally, this problem has been addressed by incorporating a gage area within which specimen thickness is reduced significantly from the value in the gripped regions. In the case of plate specimens incorporating flexures, experience has shown that thickness reduction factors as high as ten are needed to achieve acceptable performance. That is failure initiating within the gage area where stress/strain conditions are both relatively uniform and relatively well defined.

Although the above approach has been used effectively in the case of conventional structural alloys, it has proved impractical for the materials of interest in this work including: advanced metallics; polymeric matrix composites; metal and intermetallic matrix composites; and ceramic matrix composites. Problems include the unavailability of material in "large" product forms and also the difficulties associated with machining complex three-dimensional geometries in complex multiphase materials. The aim of the present work was to develop an alternative approach involving use of a simplified specimen design and use of reusable fixtures incorporating the design features needed to decouple the applied biaxial loading. A further goal was to develop fixturing and procedures which would allow in-plane biaxial tests to be conducted on a wide range of advanced materials while at the same time keeping costs within acceptable limits.

SPECIMEN DESIGN AND ANALYSIS

The current cruciform specimen design (fig. 1) developed at NASA for testing conventional structural alloys served as a starting point for this work. In the new approach, the gripped regions of the current design are replaced by four individual fixtures which incorporate slotted fingers to decouple the biaxial loading. The gage section of the current design is replaced by a specimen incorporating a reduced gage area and four sets of slots and fingers for attachment purposes. The focus of the preliminary design and analysis work was on determining whether a specimen design with this configuration would meet two straightforward design requirements. These were (1) that the maximum stress in the part should occur within the gage area, and (2) that the stress/strain distribution in the gage area should be reasonably uniform, say, within ±5 percent of the mean. Details of the conceptual design and the results of specimen design and analysis work are described in the following.

Conceptual Design

A conceptual design for the new approach is shown in figure 2. One constraint on the overall size of the assembly was that a 432×432 mm envelope is available within the load frame for installation and gripping purposes. Four slotted finger fixtures are shown attached to a specimen fabricated from a 229×229×6 mm plate. These dimensions were selected to give a relatively large gage area, 76 mm outside diameter in the case of specimens with circular gage areas. This approach was adopted primarily with instrumentation requirements in mind. The attachment method is not shown in figure 2 for simplicity of drawing.

Details of a slotted finger attachment are given in figure 3. The design shown is idealized in that no stress relieving blend radii were included so as to simplify finite element analysis of the complete assembly. This approach was acceptable because the focus of initial work was on the performance of the specimen rather than on the performance of the fixturing. The slotted finger attachments are assumed to be gripped over 152×38 mm^2 areas on both top and bottom surfaces. Earlier experiments using the current NASA cruciform specimen design had shown that this arrangement met the loading requirements of planned test programs. Experience gained in these earlier experiments was also used to size the finger and flexure configuration shown in figure 3. The four finger arrangement was an obvious choice given the need to locate a slot on the fixtures centerline and also given the need to maintain symmetry about the fixtures centerline.

Details of the initial specimen design are given in figure 4. As noted earlier, it is assumed to be fabricated from a 229×229×6 mm plate. Perhaps the most important design feature is the arrangement of slots and fingers used for attachment and loading purposes. It was recognized at the outset that the slot configuration would play a key role in obtaining an optimized specimen design. As indicated in figure 4, a slot width of 10 mm was selected for initial feasibility studies. Other dimensions shown in symbolic form were treated as variables in subsequent optimization analyses.

Stress Analysis Details

The ANSYS finite element code, version 5.4, was selected for this work, primarily because it features an optimization package. The plan was to model 1/8 of the complete assembly with the six specimen dimensions shown in figure 4 expressed as variables and to perform fully automated analyses until an optimum set of specimen dimensions had been obtained. To facilitate this process, a command input file was created using the ANSYS Parametric Design Language (APDL). This provides the means to create finite element models in terms of variables, which in turn allows for easy and rapid design changes. Approximately 1000 lines of ANSYS commands were used to define parameters, generate the finite element model, solve, evaluate results, and begin optimization looping.

As indicated earlier, external loading was applied to the assembly over 152×38 mm^2 areas. An equibiaxial stress state was introduced into the finite element model by constraining all surface nodes within the gripped regions to displace 0.127 mm in the positive sense in the two loading directions. Similarly, clamping within the specimen grips was simulated by constraining all surface nodes within the gripped region to displace 0.005 mm in the thickness sense. Regarding the attachment method, the specimen and the slotted finger fixtures were modeled as a single unit in the early analyses which focused on specimen performance. Note that the material properties used in this work were handbook values for Inconel 718 and that the results of stress analyses are expressed in the form of von Mises equivalent stress throughout.

Stress Analysis Results

The results shown in figures 5 and 6 were obtained in one of a large number of stress analyses performed during the initial stages of the research. One interesting feature of the overall deformation behavior of the assembly shown in figure 5 is the ability of the finger and flexure arrangement to accommodate large overall displacements and rotations without becoming overstressed. This flexibility is of course the mechanism by which loading in the two directions is partially decoupled. As might be expected, analysis of the results showed that stress concentrations occurred at three locations outside of the gage area. As indicated in figure 6, these locations were the center slot, the outer slot, and the fillet region. Simply stated, the optimization process involved varying specimen dimensions in a systematic manner until the

maximum stress values at these locations were less than the average stress in the gage area, say, with a 20 percent margin of conservatism.

Analysis of the data shown in figures 5 and 6 indicated that this condition had partially been achieved with the particular specimen design shown. The average and maximum stresses in the gage area were 392 and 397 MPa, respectively. The maximum stress levels in the center and the outer slots were 367 and 352 MPa, and the maximum stress in the fillet region was 382 MPa. Thus, this design met the design requirement that the maximum stress should occur within the gage area. However, it was apparent that additional work was needed to achieve the 20 percent margin of conservatism. The second design requirement was that the stress distribution in the gage area should be uniform within ±5 percent of the mean. Analysis of the data shown in figure 6 showed that the stress distribution in the gage area fell within ±2.4 percent of the mean, easily meeting the target value.

Optimization Method

The combination of specimen dimensions used in obtaining the above result was as follows:

- Gage section radius (R1) = 41.28 mm
- Center slot length (SLA) = 35.50 mm
- Outer slot length (SLB) = 37.00 mm
- Fillet radius (FR) = 27.94 mm
- Gage area thickness (T1) = 1.25 mm
- Thickness transition radius (TR1) = 12.70 mm

The optimization process followed in obtaining these results was not straightforward and proved to be extremely time-consuming. Evaluation of the various ANSYS optimization routines showed that in this application, the routines had difficulty converging on optimum sets of values. The factorial routine was found to be most useful for the present work as it allowed predetermined combinations of specimen dimensions to be investigated in a straightforward manner. As described in the following, the "automatic" process was supplemented by presenting the results of stress analysis in graphical form and by analyzing the results by hand. This approach effectively narrowed the design space and allowed optimum data sets to be determined more efficiently.

As a first step, fully automated stress analyses were conducted for up to thirty-six combinations of center and outer slot length and gage section thickness. As illustrated in figure 7, these data were plotted to establish the optimum combination of center and outer slot length. This was defined as the intersection point giving the minimum stress condition at the two slot locations. It can be seen in figure 7 that the optimum values of center and outer slot length established in this manner were 35.50 and 37.00 mm. One important result was that the curves representing stress conditions at the two slot locations and at the fillet region were found to be unaffected for the most part by changing gage area thickness. The most important effect of changing this variable was to shift the position of the gage area curve in the vertical sense relative to the stress axis. Thus, selecting the optimum gage area thickness simply involved identifying the curve that fell above the intersection point with some reasonable level of conservatism. The optimum value of gage area thickness selected in this manner was 1.25 mm.

Additional stress analyses were then conducted to determine the optimum value of fillet radius. This approach was possible because changing this variable did not have a major effect on the stress states at the slots and within the gage area. As illustrated in figure 8, these results were also plotted to determine the minimum feasible value of fillet radius which was 26.9 mm for the case shown. A value of 27.94 mm was selected as being optimum for the particular specimen design as it provided some margin of conservatism.

Final Specimen Designs

Given this encouraging result, attention was shifted to the design of gripping and attachment methods and to modifying the initial specimen design as found to be necessary. By way of background, it was anticipated that load levels as high as ±222 kN would be needed in tests planned for aeropropulsion materials of interest. Relatively simple attachment methods using bolts, for example, as the primary means of load transfer proved inadequate, primarily because of the previously noted size constraints. The approach adopted to resolve this difficulty was to incorporate tapers on the specimen fingers to allow load transfer by means of shear. This change was made reluctantly as it was viewed as introducing a major element of complexity to the specimen design. A further change was that the width of the slots was increased to reduce stress levels at the root locations and to increase margins of conservatism.

Details of the final specimen design featuring a circular gage area are given in figures 9 and 10. One change from the initial design is that the width of the fingers is reduced from 19 to 16 mm. This allowed the slot width to be increased from 10 to 14 mm. Further, an 8°00′ ±15′ taper was incorporated on the gripped section to facilitate load transfer into the specimen (fig. 10). Optimization exercises similar to those described above were conducted for two values of overall plate thickness, 19 and 25.4 mm. The optimized set of dimensions for the two thicknesses are summarized in table I, and the results of stress analyses are summarized in table II. The relative merits of the designs will be discussed later in the paper.

REUSABLE FIXTURING DESIGN AND ANALYSIS

The first objective of the fixturing design work was to identify the optimum attachment method for specimens with the slot and finger configuration described above. A number of attachment methods were considered during initial design studies and all but two rejected, primarily because of concerns regarding complexity and cost. Work on the two most promising concepts was continued through detailed design and in one case through manufacture. The preferred approach uses a yoke arrangement which has the important advantage of not requiring any further modifications to the specimen designs described earlier. The design and analysis process followed in achieving a final design is outlined as follows.

Design Details

As a first step, a number of changes were made to the slotted finger attachment (fig. 3) which served as a starting point for this work. It was recognized that the design in its original form was going to be difficult and expensive to manufacture and, with this in mind, the original unit design was broken down into nine subcomponents. These were eight fingers and a single mounting plate for assembly purposes. Details of this assembly are shown in figures 11 and 12. Here it can be seen that the mounting plate incorporates eight slots to accommodate the fingers and that setscrews are used for assembly purposes. The finger design includes tapers on two surfaces to match the corresponding tapers on the specimen and the yoke. A further design feature worth noting is the flats which were provided to ensure positive location between the end of the specimen and the fingers. An undercut was included at the same location to ensure proper specimen seating and also to provide some flexibility for specimen gripping.

The important features of the yoke gripping arrangement are shown in figures 13 to 15 where, for simplicity, a single pair of fingers is shown attached to a rectangular block. The plan was to first subject the fixturing to detailed evaluation under uniaxial loading. The prototype fixturing shown in these figures was manufactured specifically for this purpose. The primary function of the yoke fixture is to prevent the fingers separating under load and to prevent relative motion between the specimen and the fingers. Stated differently, the yoke's function is to ensure that the end of the specimen stays in full contact with the mating surfaces of the fingers under both tensile and compressive load-ings. This condition was to be achieved by effectively clamping the ends of the specimen between finger pairs by applying suitable preload to the assembly. This preloading was to be achieved using the two preload bolts in conjunction with the tapers on the mating surfaces of the fingers and the yoke. The first goal of analysis was to determine whether effective clamping could be obtained without overstressing either the bolts or the yoke. Also, the

stiffness and load transfer characteristics of the attachment method were to be investigated to establish the useful loading range available with the design.

Stress Analysis Details

The ANSYS finite element code, version 5.4, was again used for this work. The plan was to model one half of the assembly shown in figure 13 and to investigate the characteristics of the attachment method over a range of uni-axial loading conditions. The effect of simply preloading the assembly was the first loading case considered. Bolt preloading in these analyses was obtained by applying known displacements to the underside of the bolt head. Further, it was of interest to investigate how the stress state resulting from preloading was modified by the superimposition of external loading. As in earlier analyses, external loading was applied by constraining surface nodes in the gripped region to displace predetermined amounts in the loading direction. The magnitudes of these displacements were varied to simulate strength tests under both tensile and compressive loading.

As with most general-purpose finite element codes, contact elements are available within ANSYS for analyzing joints and attachments. Line contact elements were used in the present work to model the contact surfaces between the mating components. One complication with this approach is that a value of contact stiffness has to be specified up front for these nonlinear analyses. Also, it is well known that the correct choice of contact stiffness is critical in regard to the accuracy of the solution and also in regard to the time taken to converge on a solution. To address this issue, a series of preliminary analyses was conducted investigating the effect of varying contact stiffness over the range $1.776\times10'$ to 1.776×10^6 kN/mm. The highest value was selected for the final analyses as it was shown to provide reasonably accurate solutions within acceptable time periods. As would be expected, a coefficient of friction value has to be specified which is judged typical for the surface condition of the mating parts under consideration. In the absence of experimental data, a value of 0.1 was assumed for the majority of analyses and a limited number of spot checks were conducted using a value of 0.2. As in the case of the earlier work, elastic constants used in these analyses were handbook values for Inconel 718.

Stress Analysis Results

The results shown in figures 16 and 17 were obtained in one of a large number of stress analyses performed on the yoke assembly. These data were obtained using a contact stiffness of 1.776×10^6 kN/mm, a coefficient of friction of 0.2, and a bolt preload of 31.6 kN. Analysis of the results showed that the maximum stress in the yoke, 692 MPa, occurred at location (2) in figure 16. The maximum stress in the finger, 1792 MPa, occurred at location (4) in figure 17. Clearly, the preload assumed in this analysis was less than ideal since it resulted in unacceptably high stresses in both the yoke and the finger. This situation was corrected in subsequent analyses by using more realistic values of bolt preload. One result of changing this variable was to change the location of maximum stress. For example, in analyses using a bolt preload of 5.816 kN and a coefficient of friction of 0.1, the maximum stress condition occurred at location (1) in figure 16 and at location (3) in figure 17. The results of all analyses performed using a contact stiffness of 1.776×10^6 kN/mm are summarized in table III.

Stiffness and Load Transfer Characteristics

The efficiency of the yoke attachment method was investigated by generating plots of applied grip displacement versus the corresponding specimen load. Such a curve is shown in figure 18 for a bolt preload of 5.816 kN and a coefficient of friction of 0.1. As would be expected, the performance of the fixture under tensile loading is significantly different from that under compressive loading. This is because the load path between the specimen and the fingers is completely different for the two loading cases. Under tension, a minor change in slope occurs at point (A) and a major change occurs at point (B) where slippage apparently occurs. Under compression, behavior is more straightforward with a minor change in slope occurring at point (C). The above data are summarized in more quantitative form in table 4 along with results obtained for other combinations of preload and coefficient of friction.

An attempt was made to investigate the cause of the slope changes using the contact status option available with ANSYS. Using this option, the status of contacting surfaces is given in three categories:

1. Gap closed, no sliding
2. Gap closed, sliding
3. Gap open

Data of this type were determined at frequent intervals during simulated loading for both the finger/yoke interface and the specimen/finger interface. The approach adopted in analyzing the data was simply to identify any significant changes in contact status that occurred during the various stages of loading. Overall, the data did not appear reliable and proved difficult to analyze. For example, there were no obvious changes in contact status at load/displacement combinations corresponding to points (A) to (C) in figure 18. One expected result was that the status at both interfaces was predominantly category (1) for the case of preload only. Also, as expected, the status at the specimen/finger interface changed to mixed (2) and (3) almost immediately on load application as a result of specimen straining. Beyond this, the data were judged to have little value and will not be discussed further.

DISCUSSION

As noted in the introduction, the aim of this research was to develop specimen designs and fixturing which would allow in-plane biaxial tests to be conducted on a wide range of aeropropulsion materials including advanced metallics and composites. The plan was to develop optimized specimen designs with relatively simple geometries to facilitate manufacture and to keep costs within reasonable limits. Further, reusable fixturing was to be developed for specimen gripping and loading purposes which would incorporate the flexures needed to decouple the applied biaxial loading. The fixturing was to be manufactured using conventional structural alloys, again with the goal of keeping costs within acceptable limits.

Inspection of figures 9 and 10 and tables I and II shows that the goal of developing a relatively simple specimen design was met as a result of this research. The design feature which enabled this result was the arrangement of slots and fingers used for attachment and loading purposes. As expected, the geometry of the slots played a key role in obtaining optimized specimen designs. Over the course of the design process, the width of the slots was progressively increased to a final value of 14 mm with the aim of reducing stress levels at the ends of the slots. This far, the slots have been configured using a simple circular detail at the root location with ease of manufacture in mind. Clearly, the possibility exists that noncircular geometries could be used to give improved results.

Slot length also played an important role in the optimization process. It was shown that best results in terms of stress distribution at the root locations were obtained when the shorter slot was located on the specimen's centerline. It was also shown that increasing slot length caused increased stress levels at the ends of the slots and reduced stress levels at the fillet radius. Best results were obtained for slot lengths in the range 30.48 to 38.10 mm and fillet radii in the range 40.64 to 50.80 mm. Interestingly, these results applied for all the various specimen thicknesses considered. The importance of these results is that it allows some flexibility in the choice of gage area thickness (T1). For example, increased values of this variable might be preferred in test programs investigating the effects of pre-existing notches or defects.

One advantage offered by the slotted finger attachment is that the flexures are located some distance from the specimen gage area. This allows the use of generous fillet radii at the specimen corners to reduce the stress concentrations at this location. As indicated in table I, fillet radii as high as 50.80 mm were used to obtain feasible specimen designs. Such an approach is not possible with the current NASA cruciform specimen design shown in figure 1. In this case, use of large fillet radii increases the stiffness of the outermost flexures resulting in unacceptably high stress concentrations at the corner locations.

The results summarized in table I show that it is possible to develop feasible specimen designs for a range of specimen dimensions. Six designs are shown in this table with overall thicknesses of 19 and 25.4 mm and with gage area thicknesses ranging from 1.524 to 2.540 mm. One method of evaluating the various designs is to normalize the maximum stresses at the slot and fillet radius locations using the average gage area stress. This procedure was followed with the results shown in table II. The normalized

values give an indication of "margin of conservatism" and can be used to rank the various designs. Adopting this approach, review of the data showed that most favorable results were obtained for center and outer slot lengths of 30.48 and 30.78 mm. With one exception, the normalized values were 0.88 or less, giving about 10 percent design margin.

The ranking process was carried one stage further by evaluating the results for various gage area thicknesses. Best results were obtained for a 1.524 mm gage area thickness in the case of the 19 mm specimen, and for a gage area thickness of 2.032 mm in the case of the 25.4 mm specimen. The margin of conservatism for these particular designs was about 20 percent. The above result illustrates that the subject specimen design offers some flexibility in meeting the particular size requirements of test programs investigating the behavior of advanced materials.

A number of candidate specimen configurations were evaluated during the conceptual design study in addition to the single-step, circular design described this far. As summarized in appendix A, these designs featured both circular and square gage areas and both single-step and two-step reductions in gage area thickness (figs. 19 to 23). On advantage of the square gage area configuration was that it was found possible to obtain near-optimum designs using relatively long slot lengths (SLA and SLB) and relatively small fillet radii (FR). The importance of this result is that both these features facilitate specimen gripping in the reusable fixturing as greater working space is provided for the yoke fixtures. The advantage of the two-step reduction in gage area thickness was that stress concentrations in the thickness transition region were reduced significantly compared to those in single-step designs. Advantage can be taken of these characteristics in research programs where specimen manufacturing costs are not a major concern. It is planned to develop fully optimized designs in future work using the designs shown in figures 19 to 23 as a starting point.

One limiting feature of the design/optimization work outlined above is that it focused entirely on a single form of biaxial loading. This was the special case of equibiaxial tensile loading which was selected in part to simplify the optimization process. One obvious question is whether the specimen designs optimized using this form of loading can be used without modification to investigate more general forms of biaxial loading. As described in appendix B, an additional series of analyses was conducted on specimen design 3.2 to address this question. Details are given in figure 24 of the approach used to investigate behavior over a single quadrant of biaxial stress space while maintaining a reference state of stress at the specimen center. The results of these analyses are shown in figures 25 to 30 and also in tables V to VII in reduced form.

In summary, it was shown that the equibiaxial specimen design can be used without modification to investigate deformation behavior under general forms of biaxial loading. This is assuming that all measurement and observation is limited to the 25.4 mm diameter circular region at the center of the specimen. For strength and fracture tests, the situation is less straightforward since the magnitude and the location of the maximum stress in the gage area varied markedly with the type of biaxial loading. In one case, the deviation of gage area stress about the mean was as high as ±7 percent. Here, the preferred approach is to modify the test setup so as to ensure that the original design requirements are met. One interesting possibility is that minor modifications can be made to the slotted finger attachment to bring stress levels at critical locations back within acceptable limits. The obvious advantage of this approach is that it eliminates the need to modify the equibiaxial specimen design.

Turning to the design of reusable fixturing, the slotted finger attachment in its final form is shown in figures 11 and 12. One important modification was that the original unit design was broken down into nine subcomponents with the primary aim of simplifying manufacture. Subsequent to the design study, eight slotted fingers were fabricated from Inconel 718 using the electrical discharge machining (EDM) method. The wire EDM method was used to machine the somewhat complicated finger profile shown in figure 12 in a single part about 32 mm wide. This part was then cut into two 16 mm widths to form a matched pair of fingers. This approach ensured the symmetry of the finger pair about the central plane of the fixture. The obvious concern here was load alignment and the need to minimize the effects of variability in machining.

A similar issue addressed during the manufacturing exercise concerned the tolerances specified for the various tapered surfaces. As noted earlier, one important goal of the fixturing design was to ensure that the end of the specimen stays in full contact with the fingers under both tensile and compressive loading. For this condition to be achieved, analysis showed that careful attention had to be given to the taper angles specified for the mating parts. Assuming a less than perfect machining job, it was shown that

the taper angle on the finger should be less than that on the specimen and greater than that on the yoke. For simplicity, an angle of 7°30′ ±15′ was selected for both taper angles on the slotted fingers. The taper angle selected for the specimen was 8°00′ ±15′ and that selected for the yoke was 7°00′ ±15′. It remains to experimentally verify that this approach will provide the required results in terms of gripping efficiency and effective load transfer under both tensile and compressive loading.

Turning to the yoke attachment, the final design is shown in figures 13 to 15 and the results of stress analysis are shown in figures 16 and 17 and in table III. It should be noted that a single value of contact stiffness, 1.776×10^6 kN/mm, was used throughout in this work. Initial analysis focused on investigating the effect of varying bolt preload and coefficient of friction on the stress distribution in the assembly. Stress analysis results are summarized in table III for two combinations of bolt preload and coefficient of friction (μ). Here, it can be seen that for (μ) = 0.2 and bolt preload = 31.6 kN, the maximum stress in the yoke is 692 MPa and that in the finger is 1792 MPa. Since the ultimate tensile strength for Inconel 718 in aged condition is about 1448 MPa, the latter stress was known to be unrealistic. However, data for this particular combination was retained as it provided useful insight regarding the load transfer characteristics of the assembly for higher values of coefficient of friction and bolt preload.

More reasonable results were obtained for μ = 0.1 and bolt preload = 5.816 kN. For this combination, the maxi-mum stress in the yoke was 450 MPa and that in the finger was 718 MPa. These values were judged acceptable as the 0.2 percent yield strength for Inconel 718 in aged condition is about 1172 MPa. The analyses were carried one stage further by simulating the effect of specimen loading. This was done by applying a range of grip displacements in both the tensile and compressive senses. One interesting result was that superimposition of tensile loading had little effect on the bolt preload whereas compressive loading caused the bolt preload to increase by about 20 percent. Stresses in the yoke were found to increase by about 15 percent under tensile loading and to decrease by about 13 percent under compressive loading. In contrast, stress levels in the finger increased by about 22 percent for both tensile and compressive loading. The important result here is that the major component of stress in the assembly resulted from bolt preloading and that subsequent specimen loading had a relatively minor effect.

Data regarding the stiffness and load transfer characteristics of the assembly are shown in figure 18 and in table IV. Note that the data shown in this figure were determined for a coefficient of friction of 0.1 and for a bolt preload of 5.816 kN. It can be seen in figure 18 that at relatively low load levels, the initial slope for tensile loading is 91.8 kN/mm and that for compressive loading is 92.8 kN/mm. Relatively small changes in slope occurred at load (kN)/displacement (mm) combinations of 5.19/0.0559 in the case of tensile loading and 5.36/0.0584 in the case of compressive loading. The 0.150 secant modulii for the two loading directions were 88.6 and 90.33 kN/mm. Thus, the magnitude of the slope changes at points (A) and (C) are relatively small, about 5 percent on average. Under tensile loading, a major change in slope occurred at point (B) which corresponds to a load level of about 14.20 kN. Load carrying capability was lost at this point giving an upper limit on the useful range of the fixture for the particular combination of bolt preload and coefficient of friction considered. Under compressive loading, behavior was better behaved with near-linear response extending to at least 22.50 kN.

Turning to the results summarized in table IV, similar behavior to that described above was observed for higher values of coefficient of friction and preload. More specifically, for a coefficient of friction = 0.1 and a bolt preload = 11.62 kN, the initial slope in tension was 96.41 kN/mm and that in compression was 91.44 kN/mm. Further, the 0.150 secant modulus for tensile loading was 91.26 kN/mm. The magnitude of these values were very close to those determined for a bolt preload = 5.816 kN indicating that the value of initial slope is not a function of this variable. Under tensile loading, the change in slope occurred at a load (kN)/displacement (mm) combination of 12.36/0.130. Apparently, increasing bolt preload by a factor of two effectively doubled the initial linear range of the fixture. Inspection of table IV shows that this trend was not continued when bolt preload was increased to 31.64 kN for a coefficient of friction of 0.2. In this case, increasing preload did not result in any increase in the linear range. One important result here is that the stiffness characteristics of the fixturing are not a function of coefficient of friction or bolt preload. Had this been the case, the design would not have been useful for in-plane biaxial testing.

CONCLUSIONS

The following conclusions were drawn from this design study aimed at developing improved specimen designs and fixturing for in-plane biaxial testing.

1. The feasibility of using specimen designs incorporating relatively simple arrangements of slots and fingers for loading purposes was demonstrated by analysis for conventional structural alloys.
2. A number of optimized specimen designs were developed with gage area thicknesses ranging from 1.524 to 2.032 mm. These designs were suitable for investigating material behavior under equibiaxial stress states.
3. Reusable fixturing was developed incorporating an assembly of slotted fingers which provide the flexibility needed to decouple the applied biaxial loading. This assembly can be reconfigured as necessary to obtain optimum biaxial stress states in the specimen's gage area.
4. A yoke gripping arrangement was developed which facilitates specimen loading while avoiding the need for holes or other forms of discontinuity in the specimen.

FUTURE WORK

The slotted finger and yoke fixtures will be subjected to detailed experimental evaluation under uniaxial loading with the focus on stiffness and load transfer characteristics. Given a positive result, a second series of experiments will investigate the performance of the fixturing under in-plane biaxial loading.

APPENDIX A

CANDIDATE SPECIMEN DESIGNS FOR FUTURE WORK

It should be noted that a number of candidate specimen configurations were evaluated during the conceptual design study in addition to the designs described earlier. These configurations were based in part on the current NASA specimen design shown in figure 1. Features of interest here include the square gage area and the two-step reduction in gage thickness. As might be expected, the evaluation process showed that these design features had both advantages and disadvantages. One disadvantage of square gage areas is that unacceptably high stress concentrations can occur at the corners if careful attention is not given to the radii at these locations. Also, use of a two-step reduction in gage thickness was known to complicate manufacture and to lead to increased manufacturing costs. With these disadvantages in mind, work aimed at developing the most cost effective design focused almost entirely on specimens with single-step, circular gage areas (figs. 9 and 10).

The conceptual design study did however identify one important advantage of the square gage area configuration. It was found possible to obtain near-optimum designs without too much difficulty using relatively long slot lengths (SLA and SLB) and relatively small fillet radii (FR). The importance of this result is that both of these features facilitate specimen gripping in the reusable fixturing as greater working space is provided for the yoke fixtures (fig. 13). Note that these fixtures are partially located in the specimen slots when assembled with the slotted finger attachments and used for biaxial testing. With this advantage in mind, it appears that further consideration should be given to the square gage area configuration and fully optimized designs developed. A starting point for this work is the design shown in figures 19 and 20. The gage area dimensions shown were optimized during the conceptual design study and do not require further work. It remains to determine optimum values of slot length and fillet radius using the optimization procedures described earlier.

Also during the conceptual design study, the use of multistep reductions in gage area thickness was shown to offer certain advantages over single-step designs. It was shown for example that stress concentrations in the thickness transition regions can be reduced significantly using the multistep approach. Thus, advantage can be taken of this characteristic in research programs where specimen manufacturing cost is not a major factor. With this option in mind, partially optimized designs featuring two-step reductions in gage area thickness are shown for further consideration in figures 21 to 23. As before, the gage area dimensions were optimized during the conceptual design study and do not require further work. Fully optimized designs can be obtained using these designs as a starting point by determining optimum values of slot length (SLA and SLB) and fillet radius (FR). It should be noted that the two-step, square gage area configuration might give best overall performance. This is assuming that this configuration in fully optimized form does indeed allow use of long slot lengths and small fillet radii. As noted earlier, the important consideration here is ease of specimen gripping in the reusable fixturing.

APPENDIX B

SPECIMEN PERFORMANCE UNDER GENERAL FORMS OF BIAXIAL LOADING

One limiting feature of the design/optimization work described this far is that it focused entirely on a single form of biaxial loading. This was the special case of equibiaxial tensile loading. One advantage of using this type of loading was that it caused symmetrical stress states to be introduced into the specimen and associated fixturing. This simplified the optimization process by effectively reducing the number of variables involved. Regardless of such efforts, the process of developing fully optimized designs remained complex and time consuming. Given this result, it was apparent that major savings in time and effort would be realized if it could be demonstrated that the equibiaxial specimen design could be used without modification to investigate more general forms of biaxial loading. Possible issues to be addressed here included the location of the maximum stress in the assembly and also the uniformity of stress in the specimen gage area.

The specimen configuration selected for further study was specimen type 3.2, details of which are given in table I. One goal in conducting this work was to maintain a reference state of stress at the center of the specimen gage area so as to allow meaningful comparison of performance under the various loading conditions investigated. The approach adopted in achieving this goal is shown schematically in figure 24. Here it can be seen that a single value of von Mises equivalent stress, 345 MPa, was used throughout. Further, six stress ratios (θ) in the range $\pm 45°$ were selected to investigate specimen performance over a single quadrant of biaxial stress space. In the case of isotropic materials, stress states in the remaining quadrants can be inferred from the symmetry of the von Mises ellipse. The components of stress, σ_x and σ_y, corresponding to the six reference conditions were calculated in a straightforward manner using the relationships shown in figure 24 and the results of these calculations are summarized in table V. It remained to establish the grip displacements needed to achieve the reference stress states in planned finite element analyses.

As noted earlier, loading in the subject in-plane biaxial tests is introduced into specimens and associated fixturing by means of four hydraulic grips. These grips rigidly constrain the gripped region of the fixturing over 152×38 mm^2 areas (fig. 3). This was simulated in earlier finite element analyses by constraining all surface nodes in the gripped regions to displace predetermined amounts in the two loading directions. Similarly, clamping within the specimen grips was simulated by constraining all surface nodes within the gripped regions to displace 0.005 mm in the thickness sense. The plan was to use the same general approach in the present investigation. To determine the required grip displacements, it was assumed that stress components at the center of the gage area, σ_x and σ_y, are related to corresponding grip displacements, Δ_x and Δ_y, by the expressions:

$$\Delta_x = K_1 \sigma_x + K_2 \sigma_y \tag{1}$$

$$\Delta_y = K_1 \sigma_y + K_2 \sigma_x \tag{2}$$

where K_1 and K_2 are constants.

Since K_1 and K_2 were unknown, it was necessary to conduct a preliminary finite element analysis to effectively calibrate these expressions. The planned approach was to apply known grip displacements to the model and to calculate the corresponding values of σ_x and σ_y. It was then possible to solve equations (1) and (2) for K_1 and K_2.

Regarding the boundary conditions and loading used in the preliminary analysis, clamping in the rigid grips was simulated by constraining surface nodes in the gripped regions using the approach described above. Loading was introduced into the finite element model by applying a simulated grip displacement of 0.127 mm in the x sense. The condition in the y sense was "gripped" but free-to-displace in the y direction. The value of Δ_y calculated as a result of this loading was –0.0336 mm and the calculated values of σ_x and σ_y were 320MPa and –100MPa. These values along with the known value of Δ_x were substituted in Equations (1) and (2) and solved for K_1 and K_2 with the following results:

$$K_1 = 4.03688 \times 10^{-4} \text{ (mm)(MPa)}^{-1}$$

$$K_2 = 2.07884 \times 10^{-5} \text{ (mm)(MPa)}^{-1}$$

At this stage, it was possible to use equations (1) and (2) to determine the required grip displacements. These values are summarized in table V along with the target stress values. The results obtained in

subsequent finite element analyses are shown in figures 25 to 30 and in reduced form in tables V to VII. The stress components, σ_x and σ_y, determined at the center of the gage area are summarized in table V along with the target values. Comparison of the two data sets showed that the finite element results were within ±2 percent of target values in the case of σ_x and were within ±4 percent in the case of the σ_y stress component. Similarly, the values of von Mises equivalent stress were found to be within ±2 percent of the target value. These differences were judged to be acceptable for the present comparative study.

The data presented in figures 25 to 30 were used to assess the uniformity of stress over the entire specimen gage area with the results shown in table VI. As noted earlier, the optimized form of specimen 3.2 was obtained using equibiaxial, tensile loading which corresponds to stress ratio = +45.0°. Not surprisingly, the stress distribution for this loading case shown in figure 25 is highly uniform with stress levels falling within ±0.5 percent of the mean over the entire gage area. Analysis of the data shown in figures 26 to 30 showed that the deviations of stress are significantly higher for the other stress ratios. More specifically, it can be seen in table VI that the deviations for θ = 0°, 15.0°, and 30.0° fall in the range ±6 to ±7 percent. Clearly, these results do not meet the original design requirement that stresses within the gage area should be uniform within ±5 percent of the mean. As expected, a much improved situation holds for stress distributions within a 25.4 mm diameter circular region at the center of the specimen gage area. In this case, deviations of stress fall within ±1 percent of the mean for all six stress ratios. This result suggests that the equibiaxial design can be used to investigate deformation behavior under general forms of biaxial loading provided measurement and observation is limited to the central 25.4 mm diameter circular region.

In the case of experiments investigating strength and fracture behavior, the focus is more on the magnitude and the location of the maximum stress in the specimen. The results shown in figures 25 to 30 were analyzed further with this particular viewpoint in mind. In this case, stress states were analyzed along individual axes to identify the magnitude and location of the maximum stress. The results of these analyses for the x, y, and 45° axes are summarized in table VI. As expected, the location of the maximum stress is highly dependent on the loading direction or stress ratio. In the case of equibiaxial loading, θ = 45.0°, the maximum stress occurred on the 45° axis at the outside diameter of the gage area. For stress ratios of 0°, 15.0°, and 30.0°, the maximum stress location fell on the x-axis, again at the gage section outside diameter. Interestingly, this pattern of behavior was not repeated for negative stress ratios. For θ = –22.5°, the maximum stress location fell on the x-axis about 12.7 mm from the center of the specimen. In the case of θ = –45.0°, the maximum stress was located exactly at the specimen center. Clearly, the behavior described above complicates interpretation of any strength or fracture tests involving general forms of biaxial loading.

Finally, attention is shifted to stress distributions over the entire specimen including the critical fillet and slot locations. More specifically, the six locations of interest are the gage area, the fillet radius, and the center and outer slots in both the x and y directions. The maximum stress values at these locations are summarized in table VII for stress ratios in the range ±45.0° along with the average gage area stress. Note that to facilitate comparison of the data, the maximum stress values were normalized using the average gage area stress. The approach adopted in evaluating these data was to use the original design requirement that the average gage section stress should exceed stress levels at other critical locations with at least a 20 percent margin. It can be seen in table VII that this design requirement was met reasonably well for all stress ratios except θ = +45.0°. For this loading case, the design margin at the fillet radius was about 10 percent. Somewhat surprisingly this indicates that specimen design 3.2 as used in this series of analyses was not in fully optimized form. Clearly, further work is needed to identify the optimum value of fillet radius needed to give the 20 percent design margin. A further result of interest is that the equibiaxial loading case proved to be the most challenging in terms of achieving optimum stress distributions over the entire specimen.

In summary, this study showed that the equibiaxial specimen design can be used without modification to investigate deformation behavior under general forms of biaxial loading. This is assuming that all measurements and observations are limited to the 25.4 mm diameter circular region at the specimen center. It was also shown that the equibiaxial specimen design can be used for other forms of testing for stress ratios of +45.0°, 0°, –22.5° and –45.0°. This recognized that data for θ = 0° can be generated in a straightforward manner under uniaxial loading using a much simpler specimen design and test setup. For the remaining stress ratios, θ = +15.0° and +30.0°, some modifications to the test setup are necessary to meet the original design requirements. One interesting possibility is that minor modifications can be made to the slotted finger attachments to bring stress levels at critical locations back within acceptable limits. The obvious advantage of this approach is that it eliminates the need to modify the equibiaxial specimen design.

REFERENCES

1. Johnson, A.E.: "Creep Under Complex Stress Systems at Elevated Temperatures," *Proc. Instn. Mech. Engrs*, Vol. 164, No. 4, 1951, pp. 432–447.
2. Monch, E. and Galster, D.: "A Method for Producing a Defined Uniform Biaxial Tensile Stress Field," *British J. App. Phys.*, Vol. 14, 1963, pp. 810–812.
3. Pascoe, K.J. and DeVillers, J.W.R.: "Low-Cycle Fatigue of Steels Under Biaxial Straining," *Journal of Strain Analysis*, Vol. 2, No. 2, 1967, pp. 117–126.
4. Wilson, I.H. and White, D.J.: "Cruciform Specimens for Biaxial Fatigue Tests: An Investigation Using Finite Element Analysis and Photoelastic Coating Techniques," *J. Strain Analysis*, Vol. 6, 1971, pp. 27–37.
5. Pascoe, K.J.: "Low Cycle Biaxial Fatigue Testing at Elevated Temperatures," *Proc. 3rd Int. Conf Fracture*, Munich, Verein Deutscher Eisenhuttenleute, Dusseldorf, 1973, Vol. 6, paper V-524/A.
6. Hayhurst, D.R.: "A Biaxial-Tension Creep Rupture Testing Machine," *J. Str. Analysis*, Vol. 8, No. 2, 1973, pp. 119–123.
7. Parsons, M.W. and Pascoe, K.J.: "Low Cycle Fatigue Under Biaxial Stress," *Proc. Instn. Mech. Engrs.*, Vol. 188, 1974, 657–671.
8. Morrison, C.J.: "Development of a High Temperature Biaxial Testing Machine," Leicester University report, Vol. 71, No. 13, 1974.
9. Odqvist, F.K.G.: "Mathematical Theory of Creep Rupture," Oxford Mathematical Monographs, Second Edition, Clarendon Press, Oxford, 1974.
10. Weerasooriya, T.: "Fatigue Under Biaxial Loading at 565 °C and Deformation Characteristics of 2'/% Cr-1% Mo Steel," Ph.D. Thesis, University of Cambridge, Jan. 1978.
11. Duggan, M.F.: "An Experimental Evaluation of the Slotted-Tension Shear Test for Composite Materials," *Experimental Mechanics*, 1980, pp. 233–239.
12. Charvat, I.M.H. and Garrett, G.G.: "The Development of Closed Loop Servo-Hydraulic Test System for Direct Stress Monotonic and Cyclic Crack Propagation Studies under Biaxial Loading," *J. Test. Eval.*, Vol. 8, 1980, pp. 9–17.
13. Brown, M.W.: "Low Cycle Fatigue Testing Under Multiaxial Stresses at Elevated Temperature," *Measurement of High Temperature Properties of Materials*, M.S. Loveday, M.F. Day, and B.F. Dyson, Eds., HMSO, 1982, pp. 185–203.
14. Henderson, J. and Dyson, B.F.: "Multiaxial Creep Testing," *Measurement of High Temperature Properties of Materials*, M.S. Loveday, M.F. Day, and B.F. Dyson, Eds., HMSO, 1982, pp. 171–184.
15. Jones, D.L., Poulose, P.K., and Liebowitz, H.: "Effect of Biaxial Loads on the Static and Fatigue Properties of Composite Materials," *Multiaxial Fatigue, ASTM STP* 853, K.J. Miller and M.W. Brown, Eds., American Society for Testing and Materials, Philadelphia, 1985, pp. 413–427.
16. Radon, J.C. and Wachnicki, C.R.: "Biaxial Fatigue of Glass Fiber Reinforced Polyester Resin," *Multiaxial Fatigue, ASTM STP* 853, K. J. Miller and M. W. Brown, Eds., American Society for Testing and Materials, Philadelphia, 1985, pp. 396–412.
17. Found, M.S.: "A Review of the Multiaxial Fatigue Testing of Fiber Reinforced Plastics," *Multiaxial Fatigue, ASTM STP* 853, K.J. Miller and M.W. Brown, Eds., American Society for Testing and Materials, Philadelphia, 1985, pp. 381–395.
18. Brown, M.W., and Miller, K.J.: "Mode I Fatigue Crack Growth Under Biaxial Stress at Room and Elevated Temperature," *Multiaxial Fatigue, ASTM STP* 853, K.J. Miller and M.W. Brown, Eds., American Society for Testing and Materials, Philadelphia, 1985, pp. 135–152.
19. Sakane, M. and Ohnami, M.: "Creep-Fatigue in Biaxial Stress Using Cruciform Specimens," Third *Inter-national Conference on Biaxial Multiaxial Fatigue, Vol.* 2, University Stuttgart, Paper No. 46, 1989, pp. 1–18.
20. Susuki, I.: "Fatigue Damage of Composite Laminate under Biaxial Loads," *Mechanical Behavior of Materials–VI, Vol.* 2 (ICM 6), Pergamon Press, Oxford, 1991, pp. 543–548.
21. Trautman, K.-H., Doker, H., and Nowack, H.: "Biaxial Testing," *Materials Research and Engineering*, H. Buhl, Ed., Springer Verlag, Berlin, 1992, pp. 308–319.
22. Makinde, A., Thibodeau, L., and Neale, K.W.: "Development of an Apparatus for Biaxial Testing Using Cruciform Specimens," *Experimental Mechanics, Vol.* 32, 1992, pp. 138–144.

23. Demmerle, J. and Boehler, J.P.: "Optimal Design of Biaxial Tensile Cruciform Specimens," *J. of the Mechanics and Physics of Solids,* Vol. 41, No. 1, 1993, pp. 143–181.
24. Boehler, J.P., Demmerle, S., and Koss, S.: "A New Direct Biaxial Testing Machine for Anisotropic Materials," *Experimental Mechanics, Vol.* 34, 1994, pp. 1–9.
25. Wang, J.Z. and Socie, D.F.: "A Biaxial Tension-Compression Test Method for Composite Laminates," *J. of Composites Technology & Research, Vol.* 16, No. 4, Oct. 1994, pp. 336–342.
26. Masumoto, H., and Tanaka, M.: "Ultra High Temperature In-Plane Biaxial Fatigue Testing System with In-Situ Observation," *Ultra High Temperature Mechanical Testing,* R.F. Lohr, and M. Steen, Eds., Woodhead Publishing Limited, Cambridge, 1995, pp. 193–207.
27. Bartolotta, P.A., Ellis, J.R., and Abdul-Aziz, A.: "A Structural Test Facility for In-Plane Biaxial Testing of Advanced Materials," *Multiaxial Fatigue and Deformation Testing Techniques, ASTM STP* 1280, S. Kalluri and P.J. Bonacuse, Eds., American Society for Testing and Materials, 1997, pp. 25–42.
28. Trautmann, K.-H., Maldfeld, E., and Nowack, H.: "Crack Propagation in Cruciform IMI 834 Specimens Under Variable Biaxial Loading," *Multiaxial Fatigue and Defonnation Testing Techniques,* ASTM STP 1280, S. Kalluri and P.J. Bonacuse, Eds., American Society for Testing and Materials, 1997, pp. 290–309.
29. Dalle Donne, C., and Doker, H.: "Plane Stress Crack Resistance Curves of an Inclined Crack Under Biaxial Loading," *Multiaxial Fatigue and Deformation Testing Techniques,* ASTM STP 1280, S. Kalluri and P.J. Bonacuse, Eds., American Society for Testing and Materials, 1997, pp. 243–263.

TABLE I.—SUMMARY OF SPECIMEN TYPES AND OPTIMIZED SPECIMEN DESIGNS

Specimen details	Specimen type	Optimized specimen dimensions, mm					
		T1	T2	SLA	SLB	FR	R1
Design with 19 mm overall thickness, and 14 mm slot width	2.1	1.524	6.35	35.56	36.45	40.64	44.45
	2.2	1.524	6.35	30.48	30.78	50.80	44.45
	2.3	2.032	6.35	30.48	30.78	50.80	44.45
Design with 25.4 mm overall thickness, and 14 mm slot width	3.1	2.032	12.70	35.56	36.45	40.64	48.46
	3.2	2.032	12.70	30.48	30.78	45.72	48.46
	3.3	2.540	12.70	30.48	30.78	45.72	48.46

Note: L1 = 80.65 mm and TR1 = 25.4 mm throughout.

TABLE II.—SUMMARY OF STRESS RESULTS AT CRITICAL LOCATIONS FOR OPTIMIZED SPECIMEN DESIGNS

Specimen details	Specimen type	Von Mises equivalent stress at location shown							
		Gage section, average		Center slot, maximum		Outer slot, maximum		Fillet radius, maximum	
		MPa	Normalized	MPa	Normalized	MPa	Normalized	MPa	Normalized
Design with 19 mm overall thickness, and 14 mm slot width	2.1	361 (±2.7%)	1	326	0.90	330	0.92	346	0.96
	2.2	352 (±1.9%)	1	288	0.82	271	0.77	299	0.85
	2.3	317 (±2.0%)	1	268	0.85	270	0.85	297	0.94
Design with 25.4 mm overall thickness, and 14 mm slot width	3.1	316 (±2.6%)	1	293	0.93	293	0.93	272	0.86
	3.2	305 (±2.4%)	1	253	0.83	248	0.81	249	0.82
	3.3	283 (±2.8%)	1	241	0.85	248	0.88	248	0.88

Notes: (1) Values in brackets are % deviations about the mean; (2) Normalization of Von Mises equivalent stress obtained using average gage section stress.

TABLE III.—STRESS ANALYSIS RESULTS FOR THE YOKE GRIPPING ARRANGEMENT

Coefficient of friction	Bolt preload, kN	Grip displacement, mm	Bolt load, kN	Specimen force, kN	Maximum yoke stress, MPa	Maximum finger stress, MPa
0.1	5.816 (0.381 mm)[5]	0	5.816	0	450 (1)	718 (3)
		0.152	5.790	12.725	450 (1)	763 (3)
		0.254	6.016	17.298	519 (1)	830 (3)
		–0.152	6.966	–14.140	411 (1)	826 (3)
		–0.254	6.962	–23.000	394 (1)	909 (3)
0.2	31.60 (0.762mm)	0	31.600	0	692 (2)	1792 (4)
		0.152	31.620	12.721	704 (2)	1772 (4)
		0.254	31.620	21.760	709 (2)	1765 (4)

Note: (1) and (2) see figure 15 for maximum stress locations in yoke; (3) and (4) see figure 16 for maximum stress locations in finger; (5) corresponding bolt head displacement in mm.

TABLE IV.—STIFFNESS AND LOAD TRANSFER CHARACTERISTICS OF THE YOKE GRIPPING ARRANGEMENT

Coefficient of friction	Bolt preload, kN	Maximum grip displacement, mm	Initial slope, kN/mm	0.150 secant modulus, kN/mm	Limit of proportionality load (kN)/displacement (mm)
0.1	5.816 (0.381 mm)[2]	0.254	91.8	88.6	5.19/0.0559
		–0.254	92.8	90.3	5.36/0.0584
	11.62 (0.762mm)	0.381	96.4	91.26	12.36/0.130
		–0.351	91.44	(1)	(1)
0.2	31.64 (0.762mm)	0.254	93.93	92.15	11.04/0.119

Note: (1) discontinuities in the load versus displacement data prevented determination of these values; (2) corresponding bolt head displacements in mm

TABLE V.—GRIP DISPLACEMENTS GIVING REQUIRED COMBINATION OF STRESS RATIO (θ) AND VON MISES EQUIVALENT STRESS ($\bar{\sigma}$) AT CENTER OF GAGE SECTION

Stress ratio, θ	Calculated values				Finite element results		
	σ_x, MPa	σ_y, MPa	Δ_x, mm	Δ_y, mm	σ_x, MPa	σ_y, MPa	σ, MPa
45.0	345	345	0.146329	0.146329	352	352	352
30.0	397	229	0.164821	0.100635	403	235	351
15.0	385	103	0.157353	0.049581	389	107	348
0	345	0	0.139167	0.007163	347	2	346
–22.5	274	–113	0.108153	–0.040107	272	–114	343
–45.0	199	–199	0.076225	–0.076225	195	–202	344

Note: σ_x, σ_y are target stress components at center of gage section. Δ_x, Δ_y are corresponding grip displacements in the x, y directions.

TABLE VI.—SUMMARY OF STRESS STATES IN GAGE AREA FOR GENERAL FORMS OF BIAXIAL LOADING

Stress ratio, Θ	Overall variation of stress in gage area		Stress states along individual axes						Maximum overall stress and location, MPa
	Average, MPa	Deviation, percent	X-axis		Y-axis		45°-axis		
			Maximum, MPa	Average, MPa	Maximum, MPa	Average, MPa	Maximum, MPa	Average, MPa	
45.0	354	±0.5	355	353	355	353	356	354	356 MPa at OD on 45° axis
30.0	347	±6.0	366	358	353	341	353	351	366 MPa, at OD on X-axis
15.0	340	±7.0	364	354	348	332	348	346	364 MPa at OD on X-axis
0	336	±6.0	356	349	347	331	343	343	356 MPa at OD on X-axis
–22.5	332	±3.0	343	342	343	332	343	341	343 MPa, 12.7 mm from center on X-axis
–45.0	336	±3.0	344	336	344	336	344	341	344 MPa at center of gage area

TABLE VII.—STRESS STATES AT CRITICAL SPECIMEN LOCATIONS FOR GENERAL FORMS OF BIAXIAL LOADING

Stress ratio, Θ	Average gage area stress, MPa	Maximum stress values at locations shown				
		Fillet radius, MPa	X-direction slots		Y-direction slots	
			Center, MPa	Outer, MPa	Center, MPa	Outer, MPa
45.0	354 (1.0)	316 (0.89)	289 (0.82)	291 (0.82)	289 (0.82)	291 (0.82)
30.0	347 (1.0)	292 (0.84)	292 (0.84)	298 (0.86)	232 (0.67)	230 (0.66)
15.0	340 (1.0)	234 (0.69)	255 (0.75)	263 (0.77)	153 (0.45)	148 (0.44)
0	336 (1.0)	193 (0.57)	206 (0.61)	215 (0.64)	81 (0.24)	75 (0.22)
–22.5	332 (1.0)	151 (0.45)	129 (0.38)	154 (0.46)	9 (0.03)	26 (0.08)
–45.0	336 (1.0)	105 (0.81)	63 (0.19)	88 (0.26)	76 (0.23)	86 (0.26)

Note: Values in brackets are normalized stresses obtained using the average gage area stress.

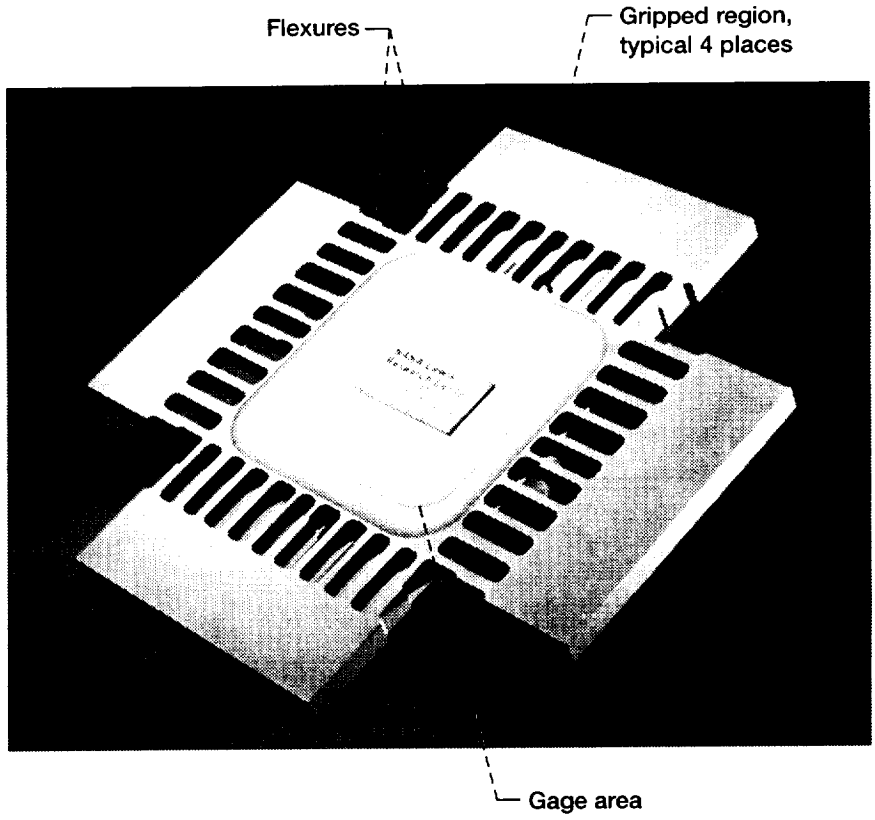

Figure 1.—Current NASA specimen design.

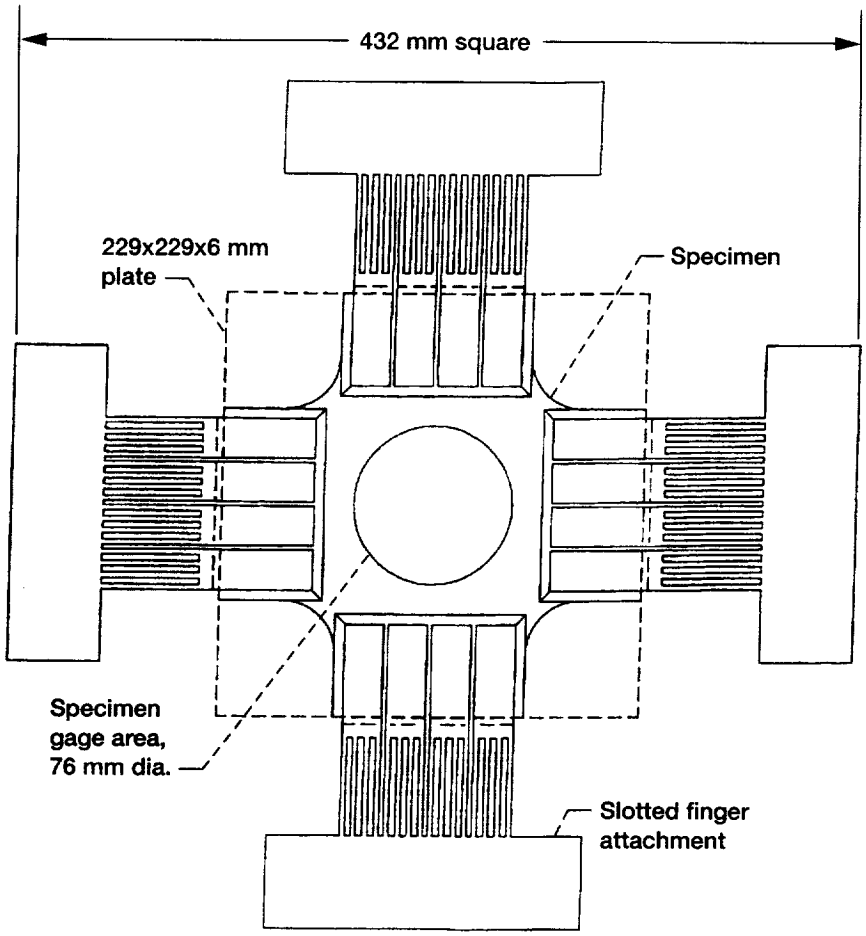

Note: Attachment method not shown for simplicity of drawing.

Figure 2.—Proposed test setup using simplified specimen design and reusable fixturing.

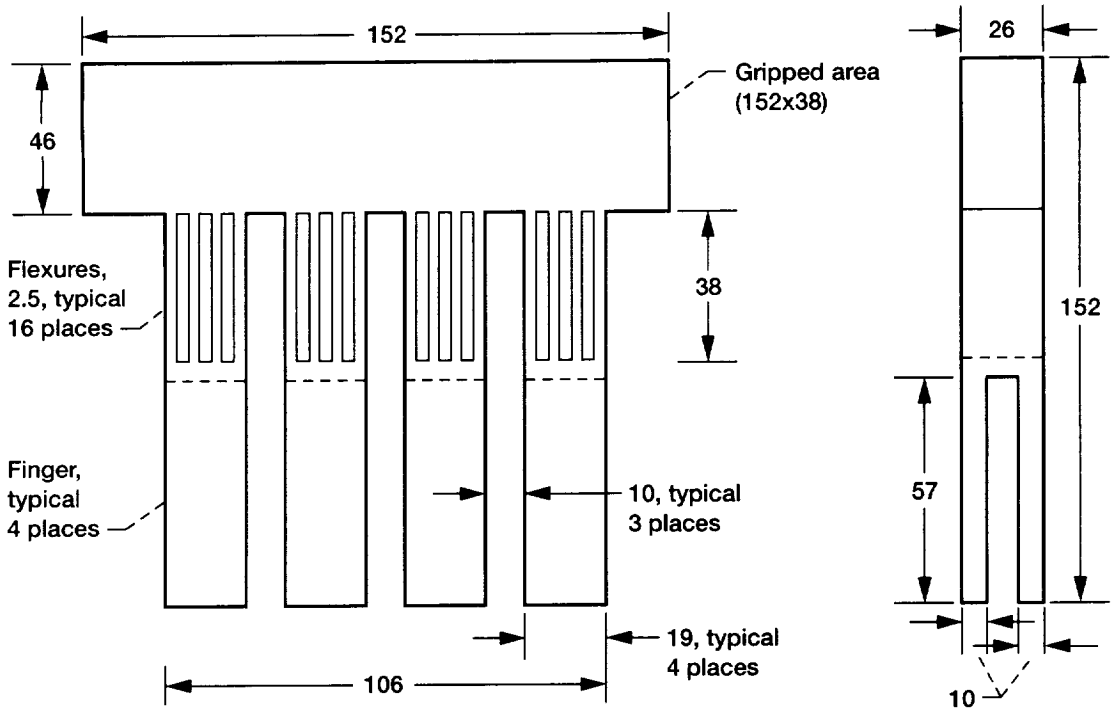

Note: All dimensions in millimeters.

Figure 3.—Slotted finger attachment: Initial design.

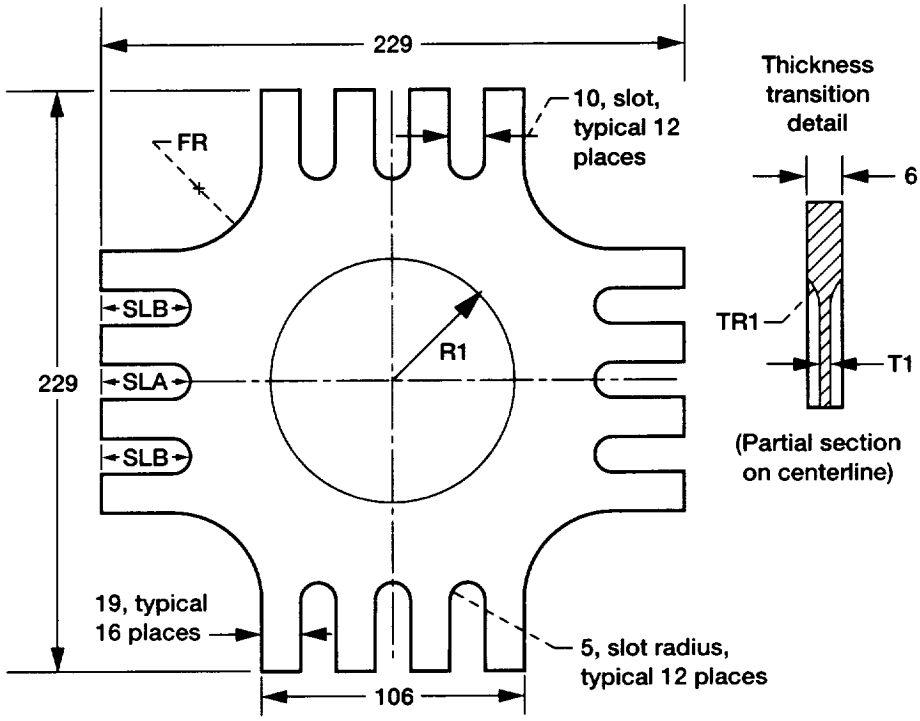

Note: All dimensions in millimeters.

Figure 4.—Conceptual specimen design with circular gage area.

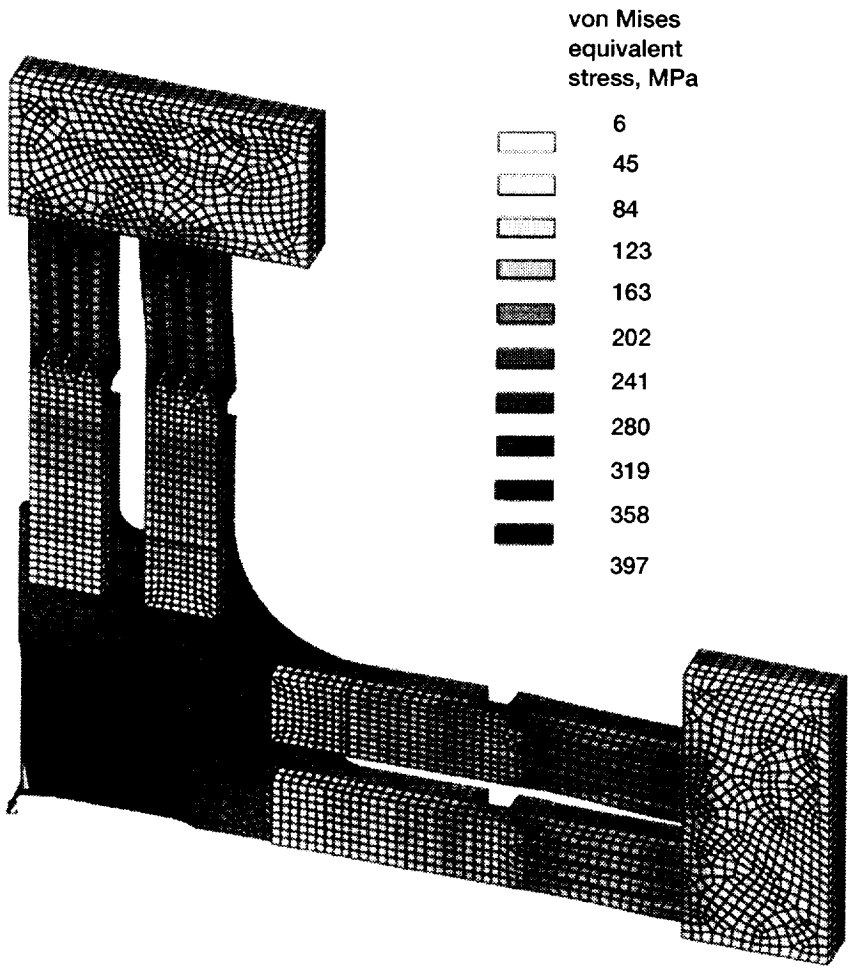

Figure 5.—Stress distribution in assembly.

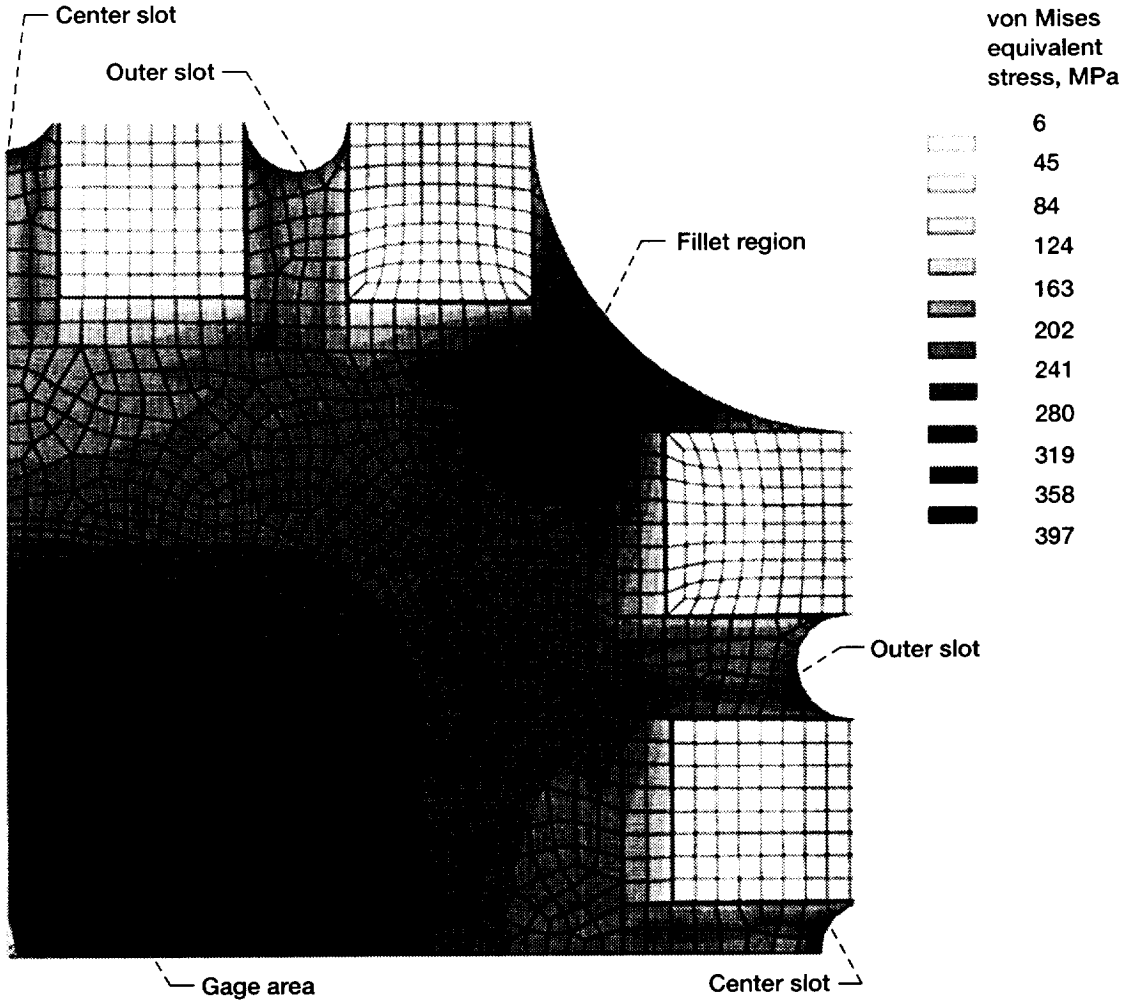

Figure 6.—Stress distribution in specimen.

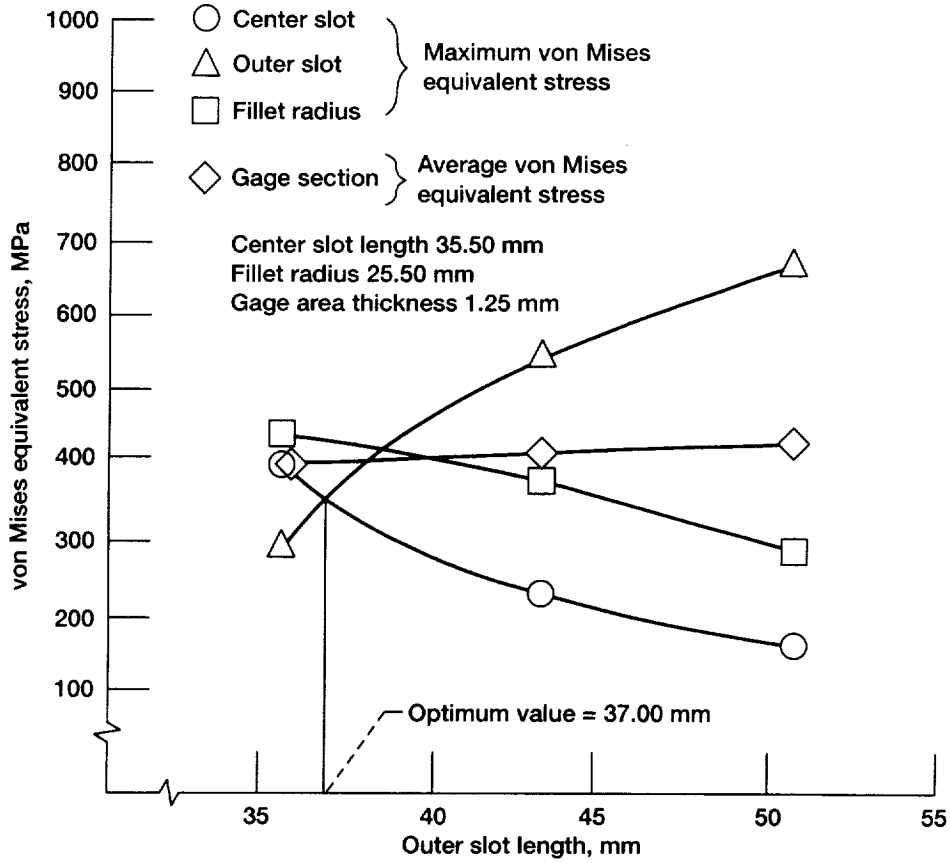

Figure 7.—Determination of optimum value of outer slot length.

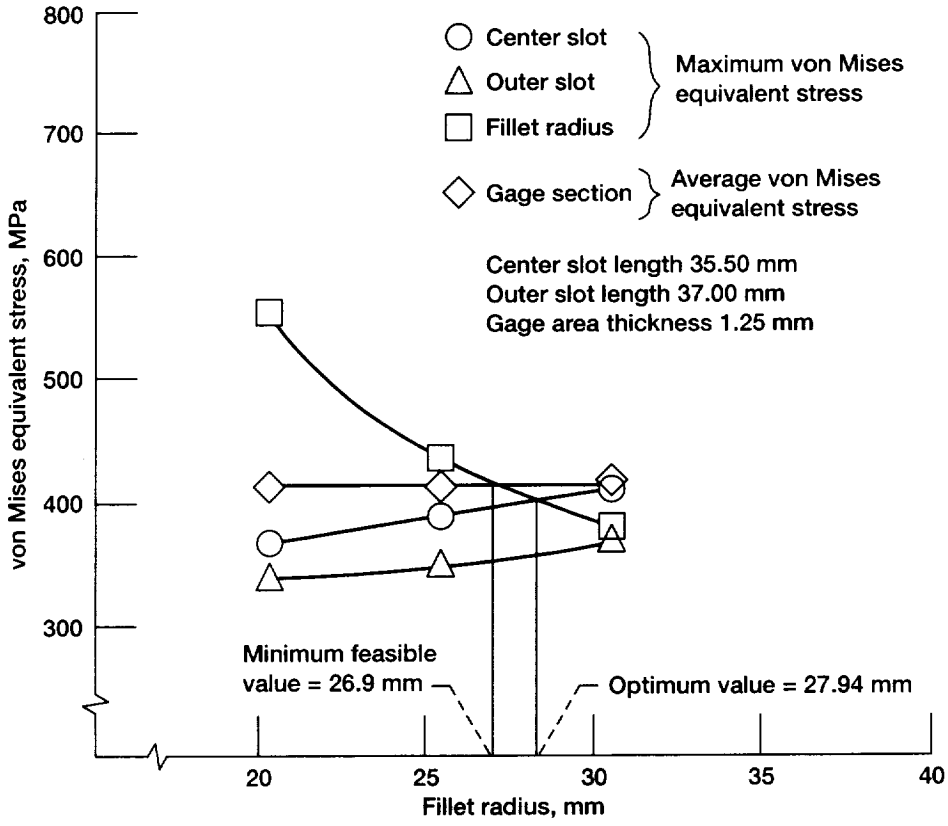

Figure 8.—Determination of optimum value of fillet radius.

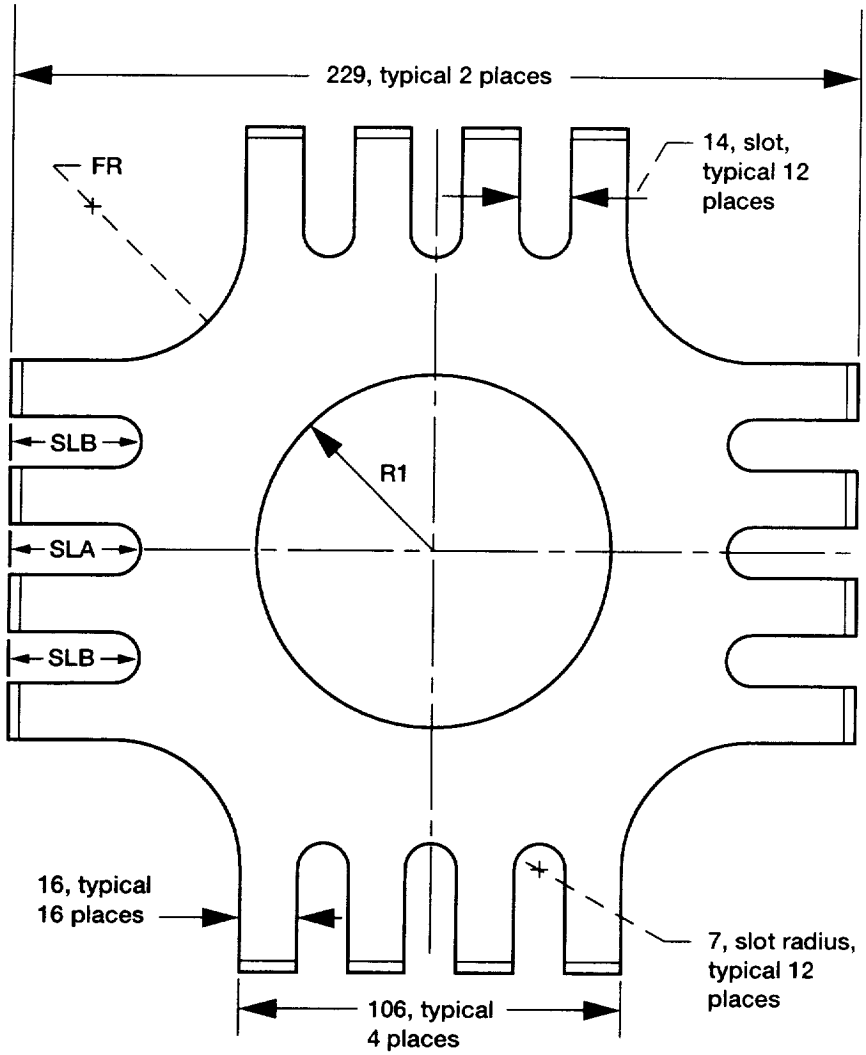

Note: All dimensions in millimeters.

Figure 9.—Final specimen design with circular gage area: Plan view.

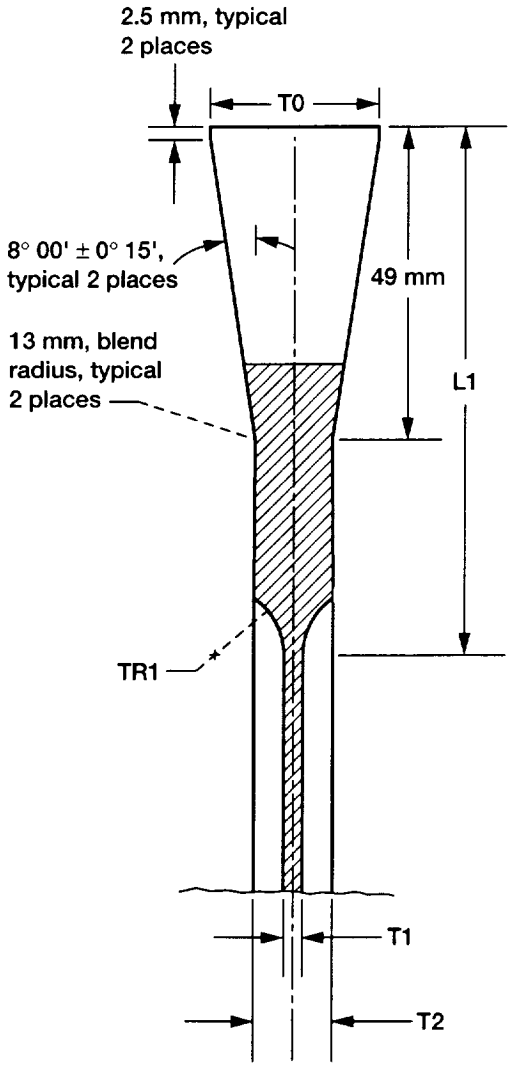

Figure 10.—Final specimen design with circular gage area: Partial section on centerline.

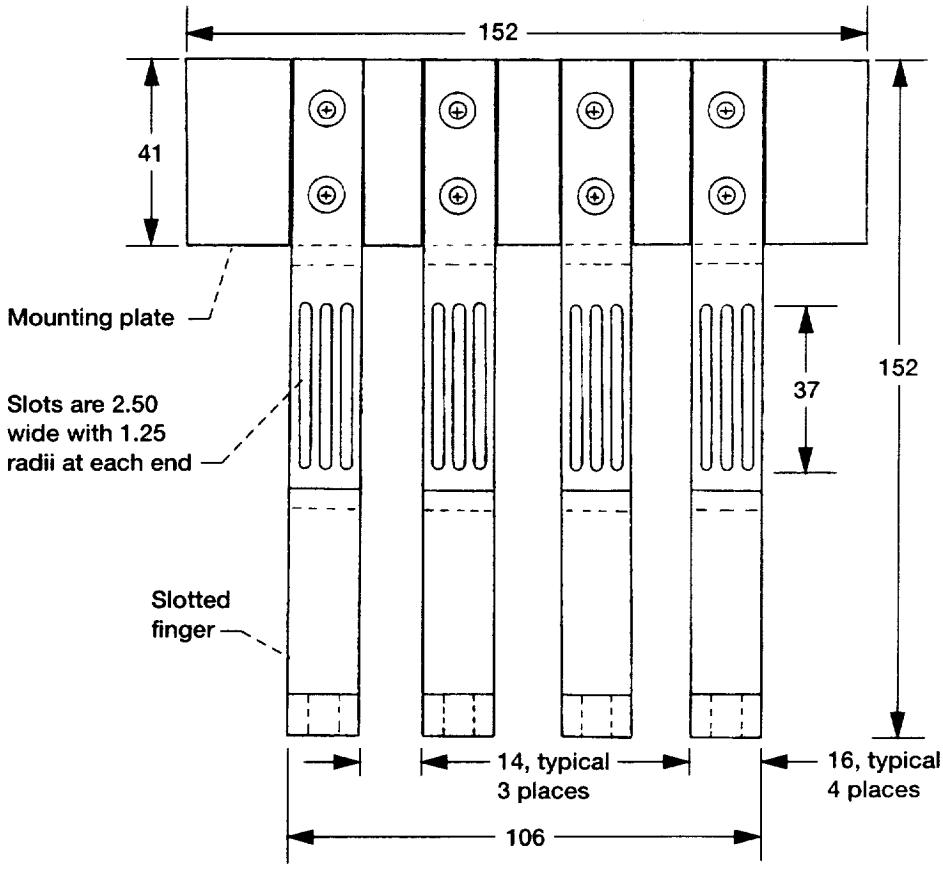

Note: All dimensions in millimeters.

Figure 11.—Slotted finger attachment: Plan view.

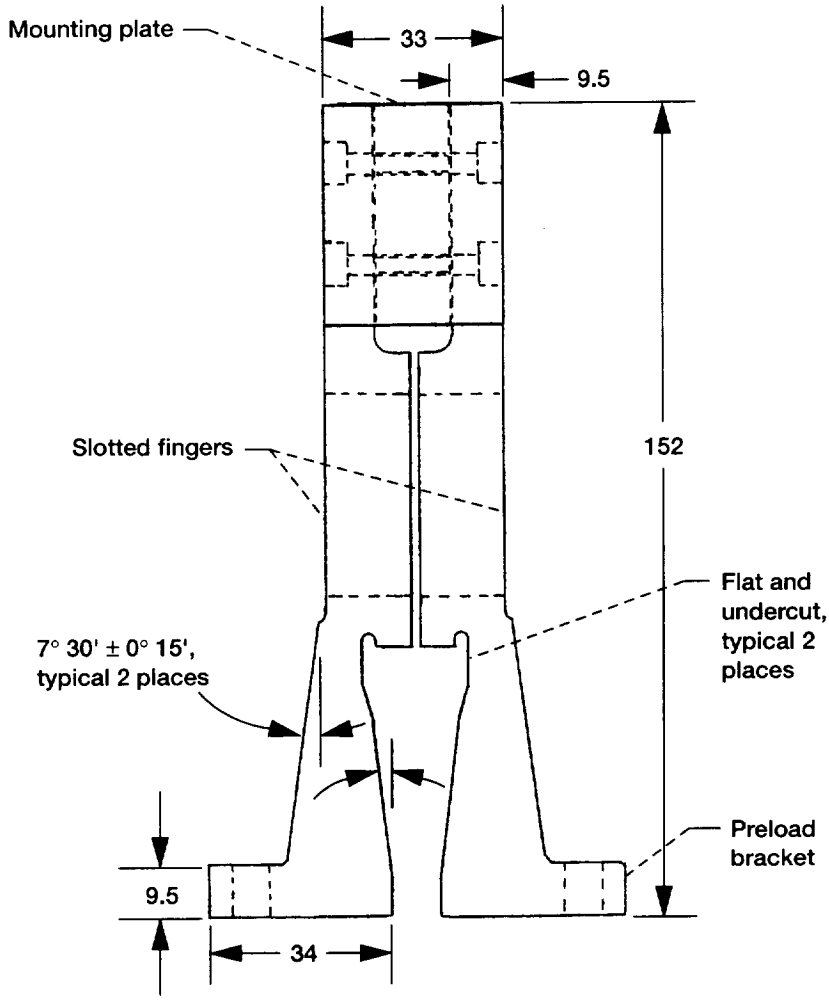

Note: All dimensions in millimeters.

Figure 12.—Slotted finger attachment: Side view.

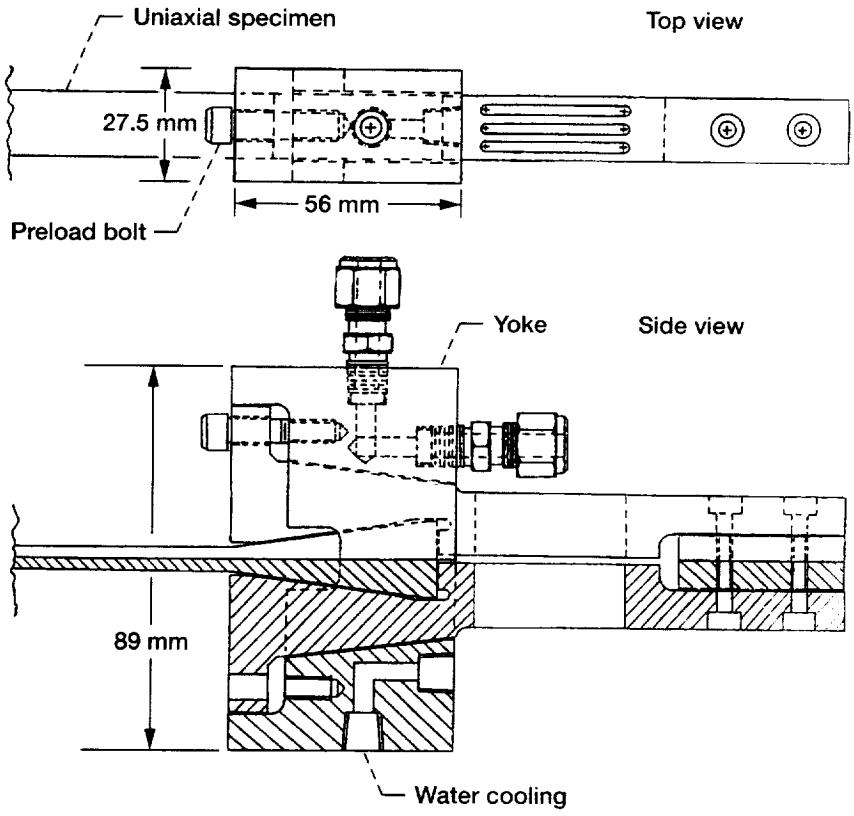

Note: Taper angle on yoke = 7° 00' ± 0° 15'.

Figure 13.—Yoke gripping arrangement and setup for evaluation under axial loading.

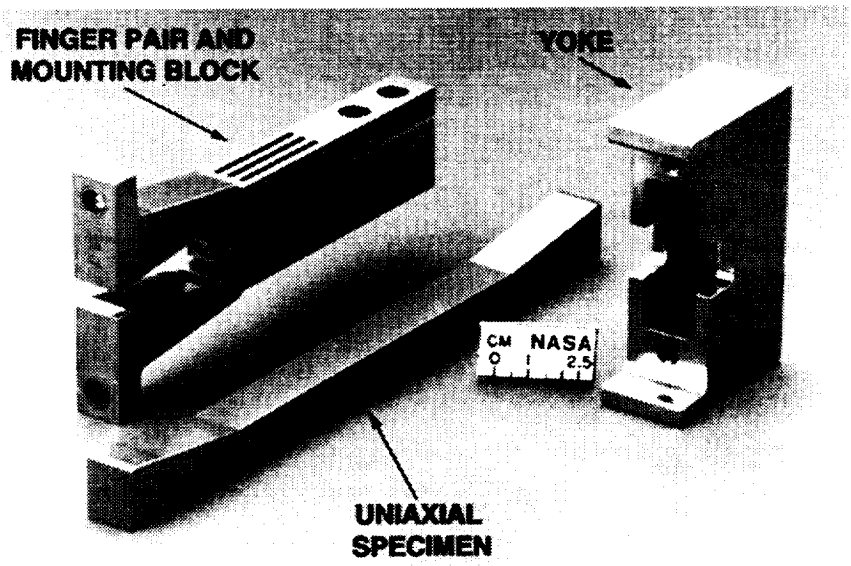

Figure 14.—Prototype fixturing in partially disassembled form.

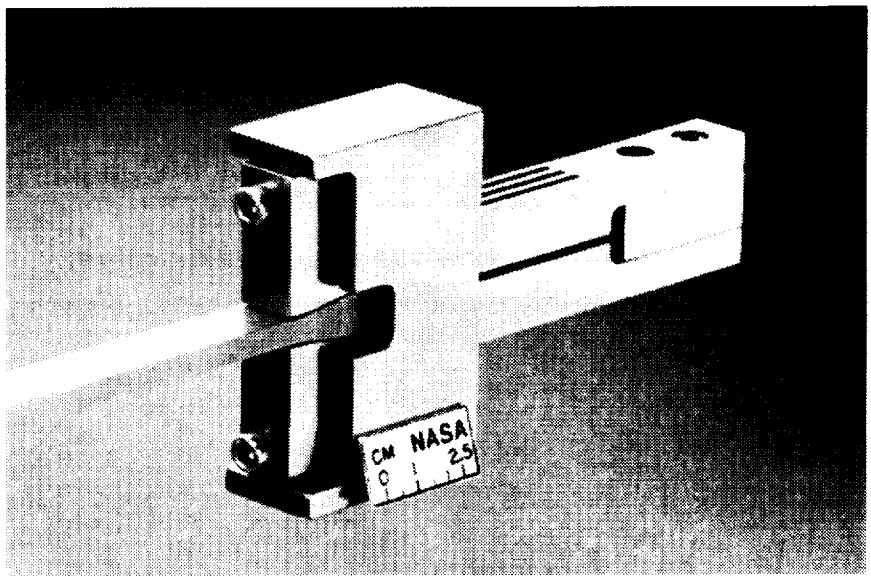

Figure 15.—Prototype fixturing in assembled form.

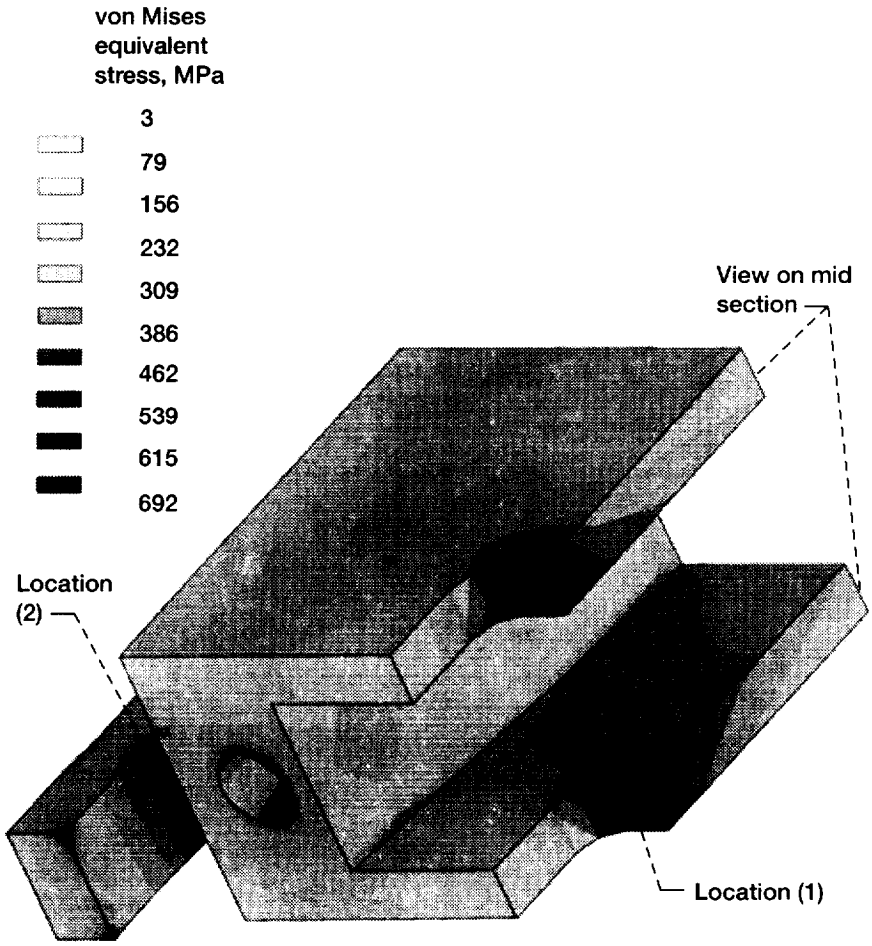

Note: Assumed coefficient of friction = 0.2 and grip displacement = 0.

Figure 16.—Stress distribution in central section of yoke for 31.6 kN bolt pre-load.

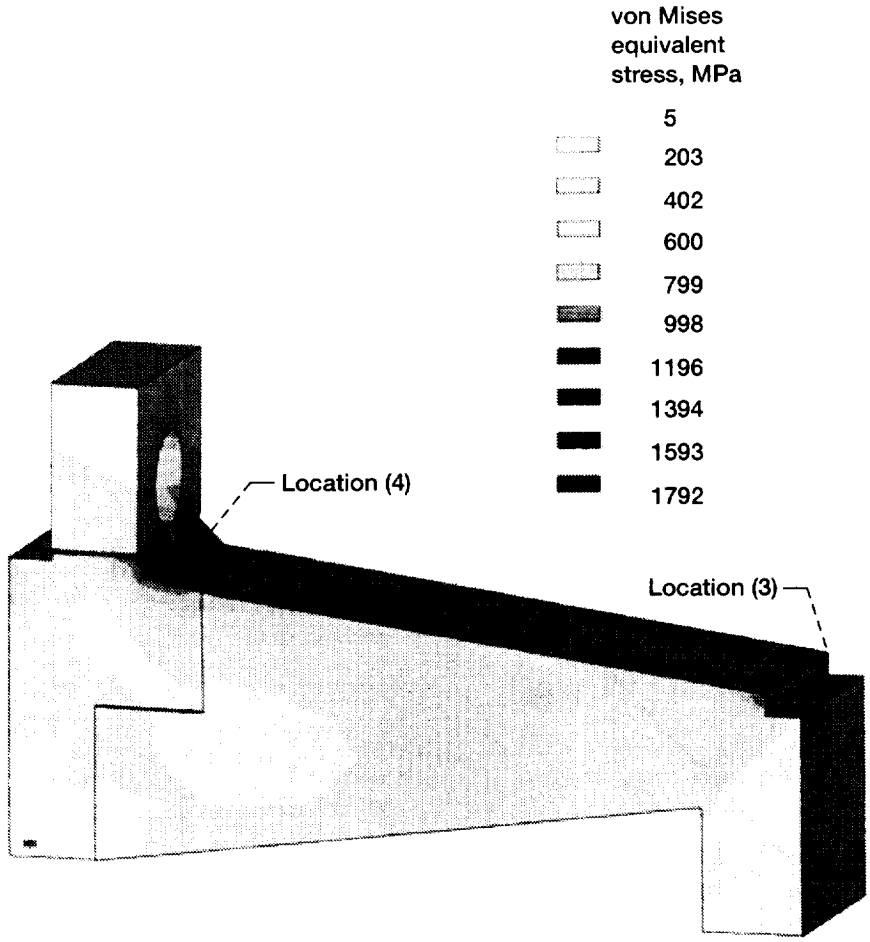

Note: Assumed coefficient of friction = 0.2 and grip displacement = 0.

Figure 17—Stress distribution in tapered section of finger for 31.6 kN bolt preload.

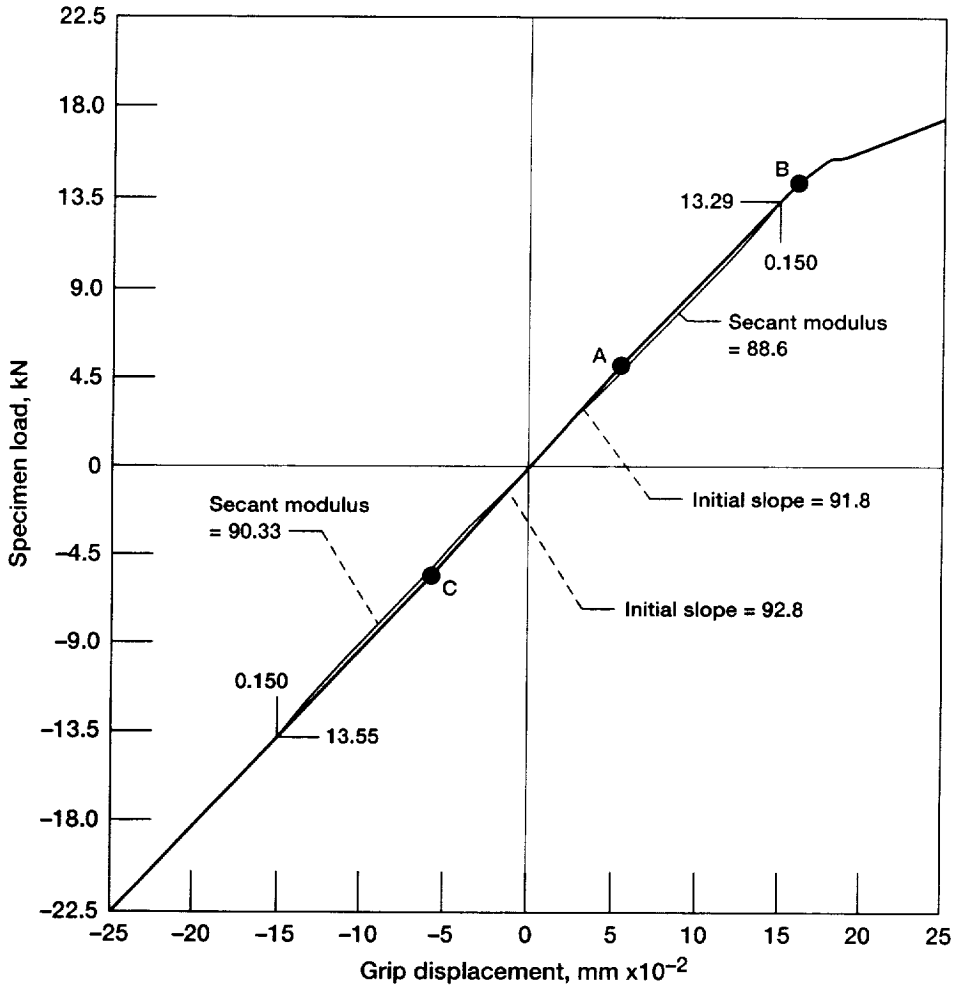

Note: Assumed coefficient of friction = 0.1 and bolt preload = 5.816 kN.

Figure 18.—Stiffness and load transfer characteristics under tensile and compressive loading.

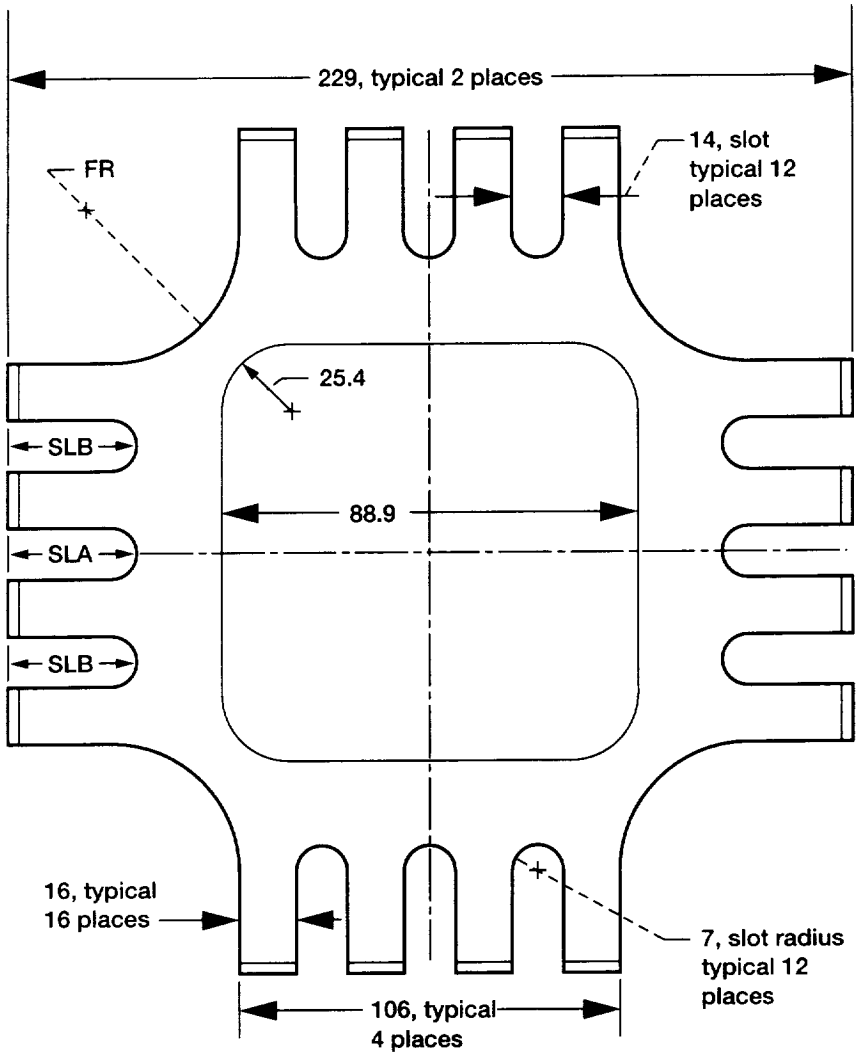

Note: All dimensions in millimeters.

Figure 19.—Specimen design with square gage area: Plan view.

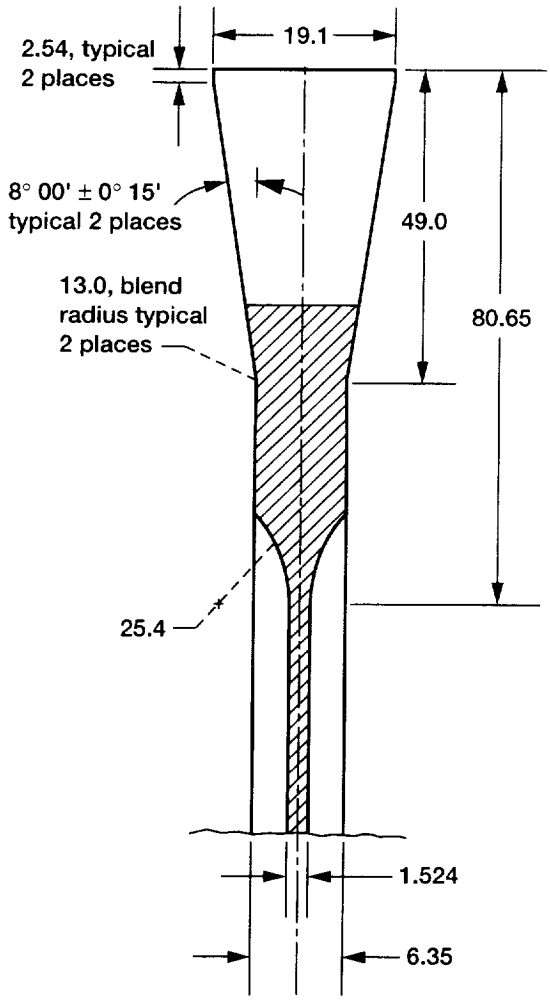

Note: All dimensions in millimeters.

Figure 20.—Specimen design with square gage area: Partial section on centerline.

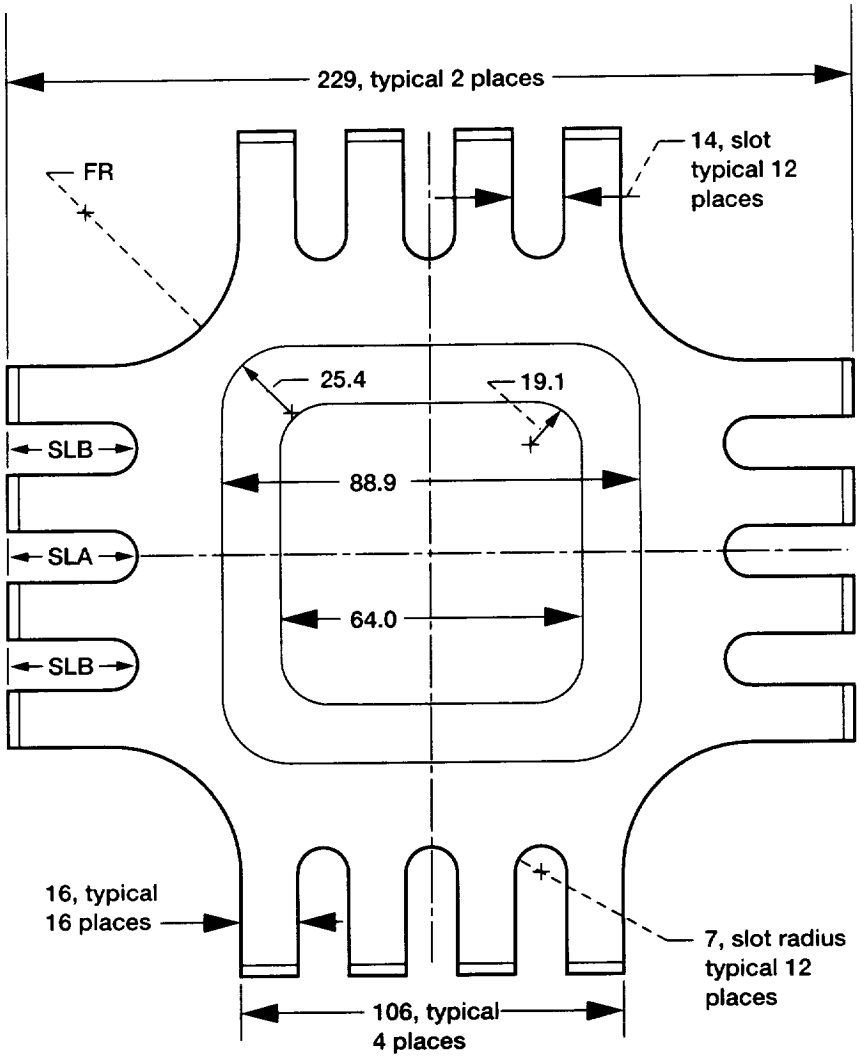

Note: All dimensions in millimeters.

Figure 21.—Specimen design with two-step square gage area: Plan view.

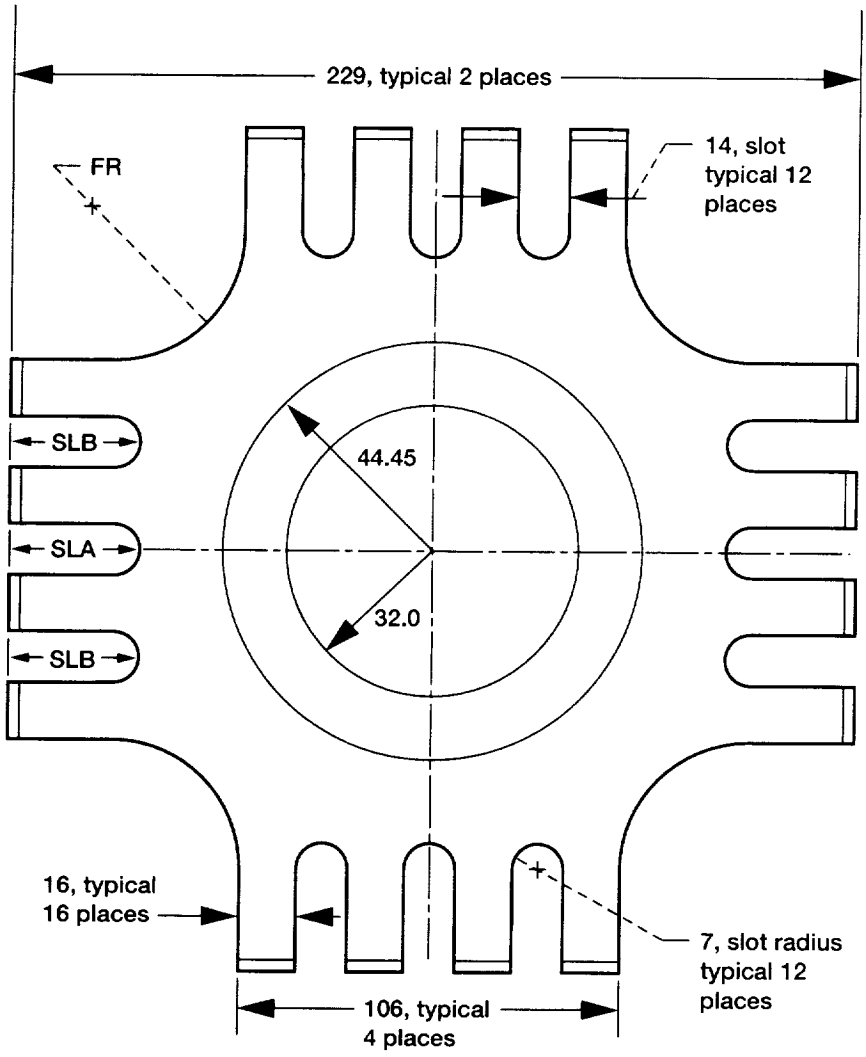

Note: All dimensions in millimeters.

Figure 22.—Specimen design with two-step circular gage area: Plan view.

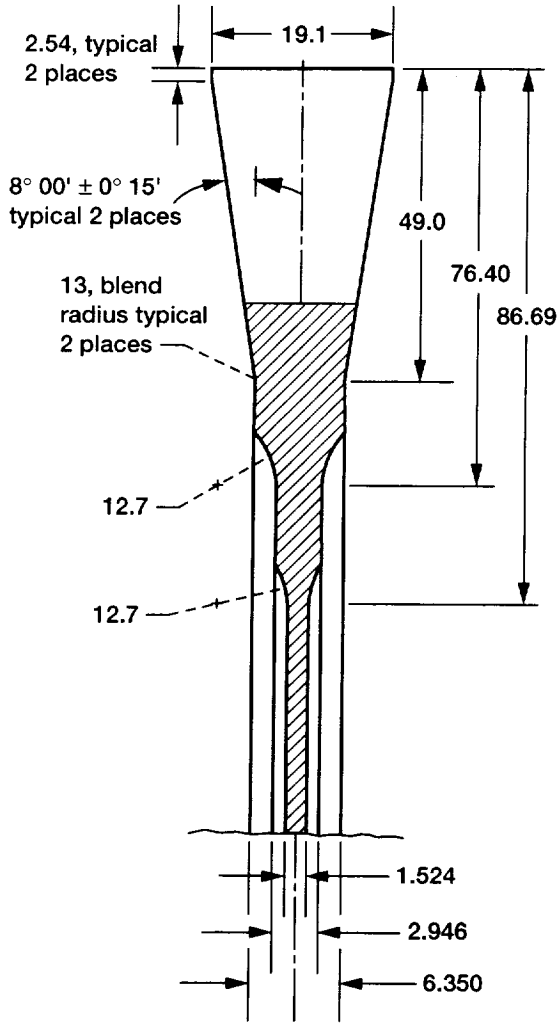

Note: All dimensions in millimeters.

Figure 23.—Specimen design with two-step gage areas: Partial section on centerline.

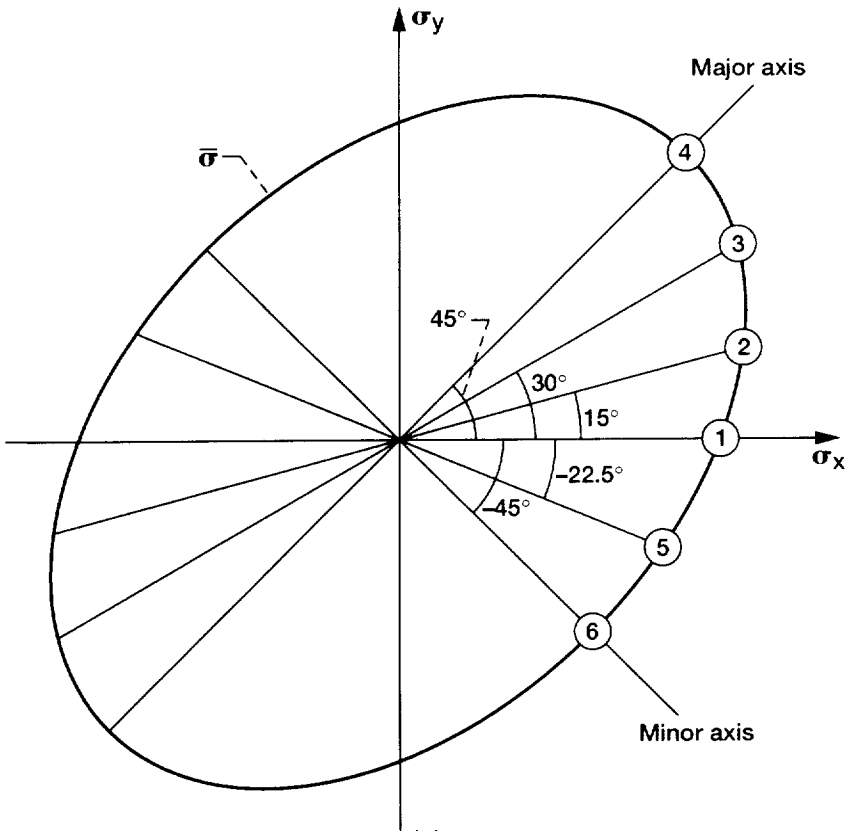

Where von Mises equivalent stress ($\bar{\sigma}$)
$= (\sigma_x^2 - \sigma_x \sigma_y + \sigma_y^2)^{1/2} = 345$ MPa

and stress ratio (θ)
$= \tan^{-1} (\sigma_y/\sigma_x)$

Figure 24.—Stress ratios (θ) used to investigate general forms of biaxial loading.

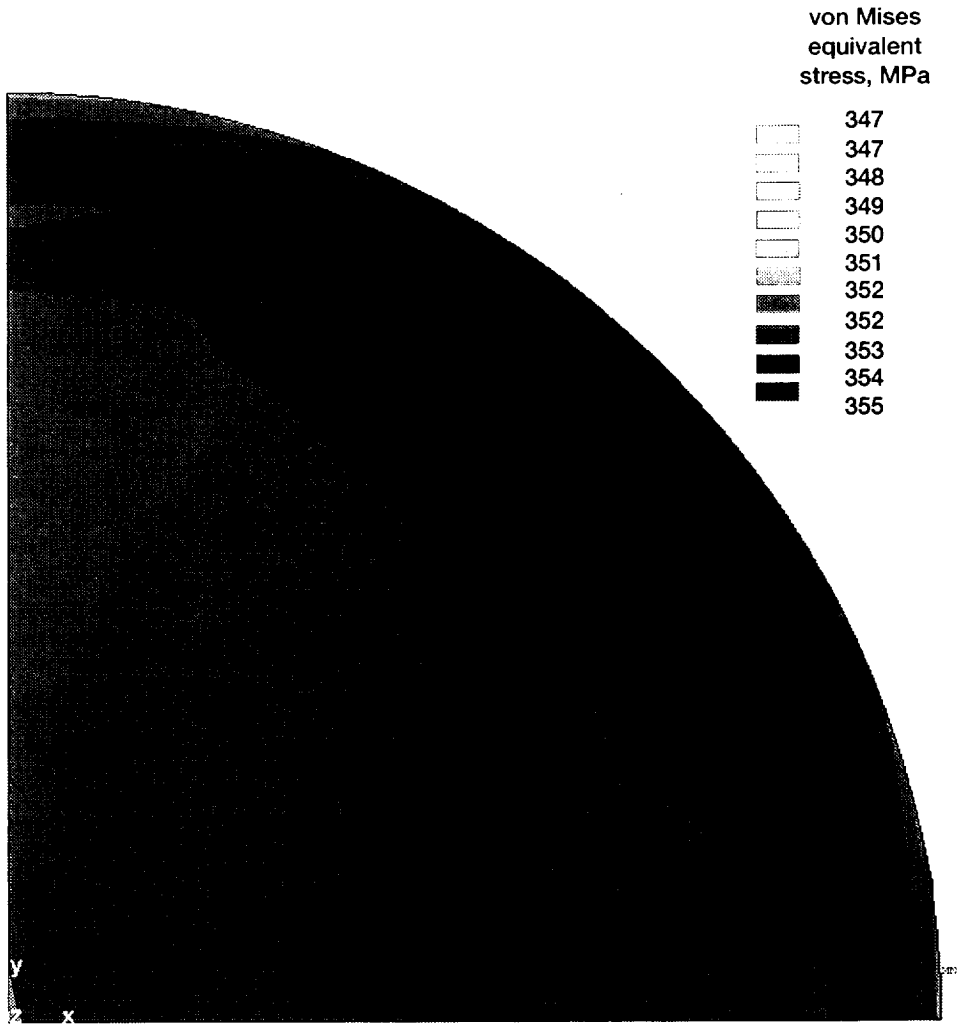

Figure 25.—Stress distribution in specimen gage area: Stress ratio (θ) = 45°.

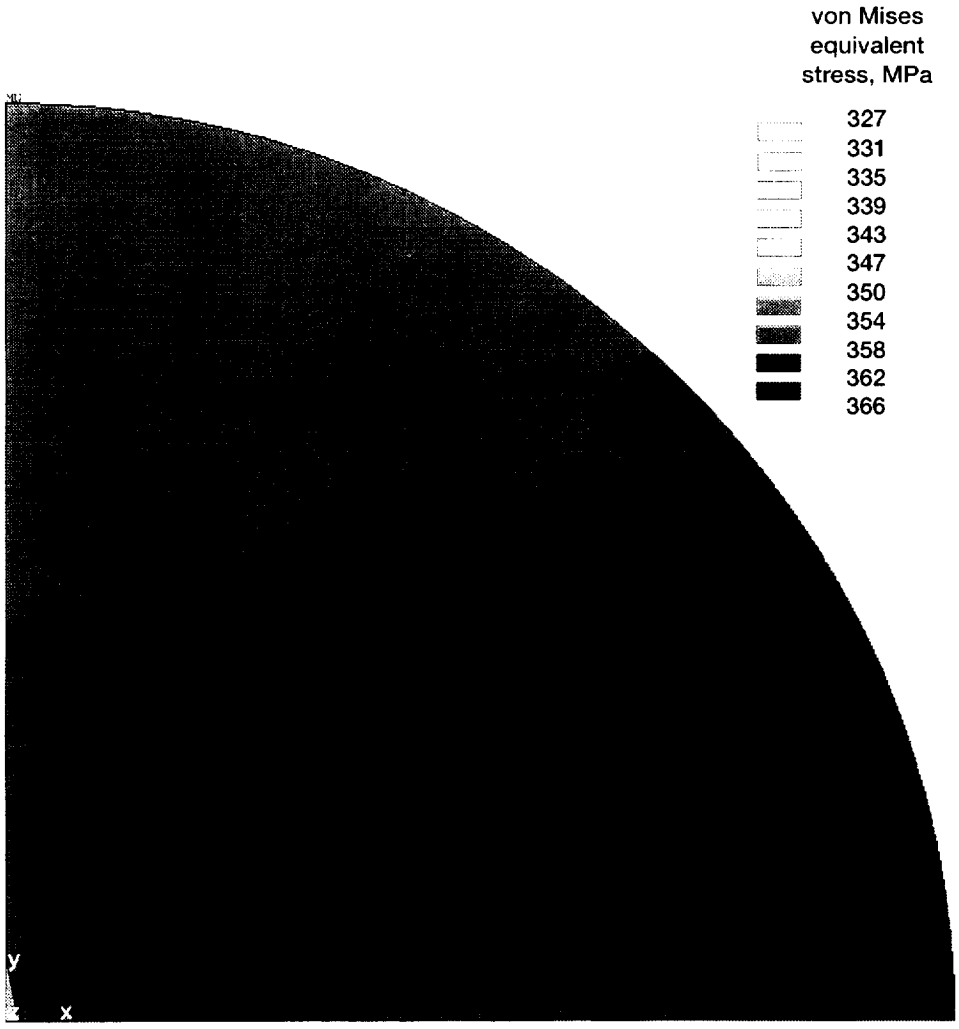

Figure 26.—Stress distribution in specimen gage area: Stress ratio (θ) = 30°.

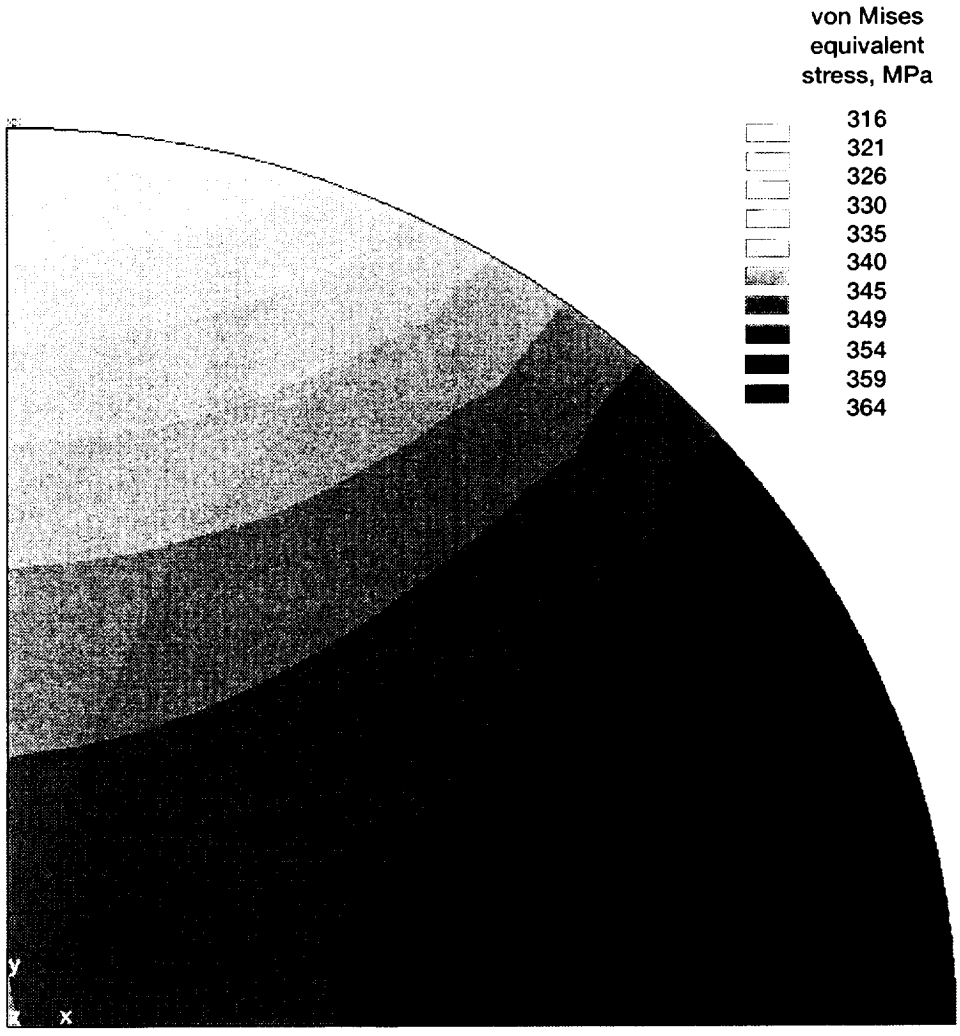

Figure 27.—Stress distribution in specimen gage area: Stress ratio (θ) = 15°.

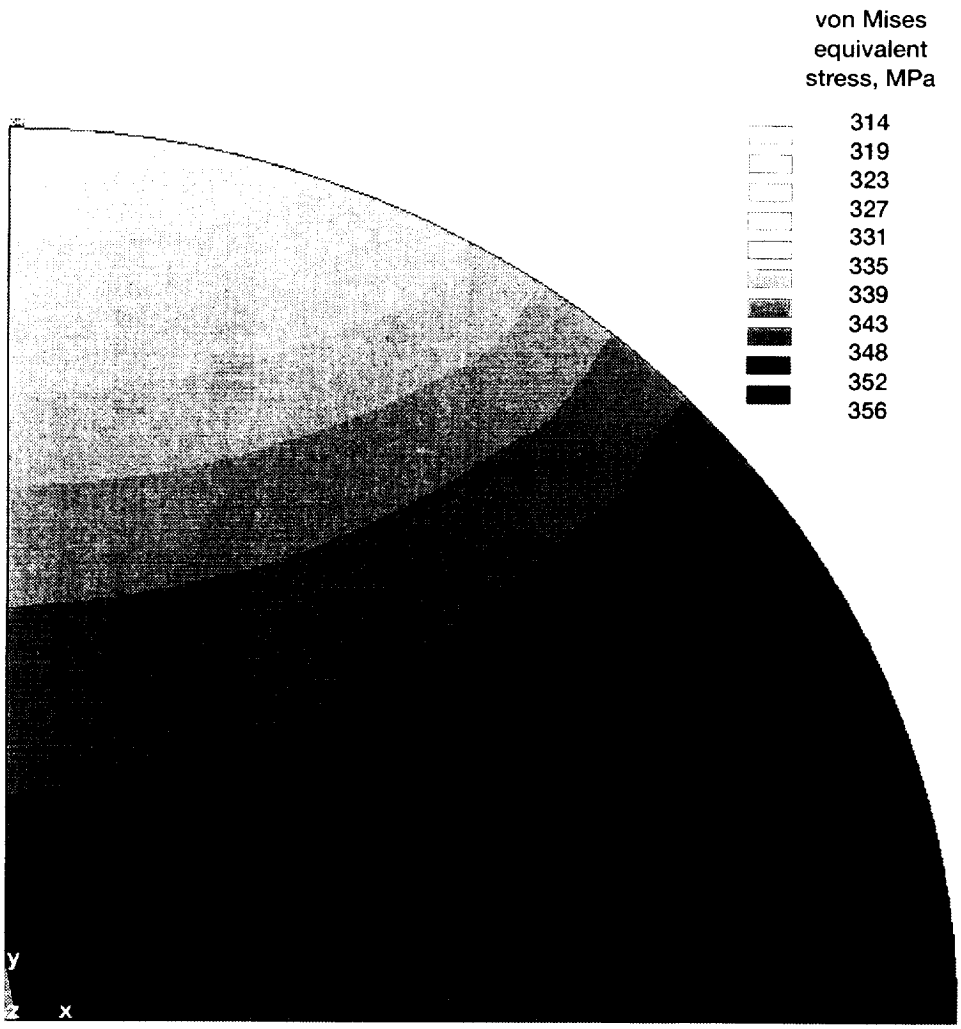

Figure 28.—Stress distribution in specimen gage area: Stress ratio (θ) = 0°.

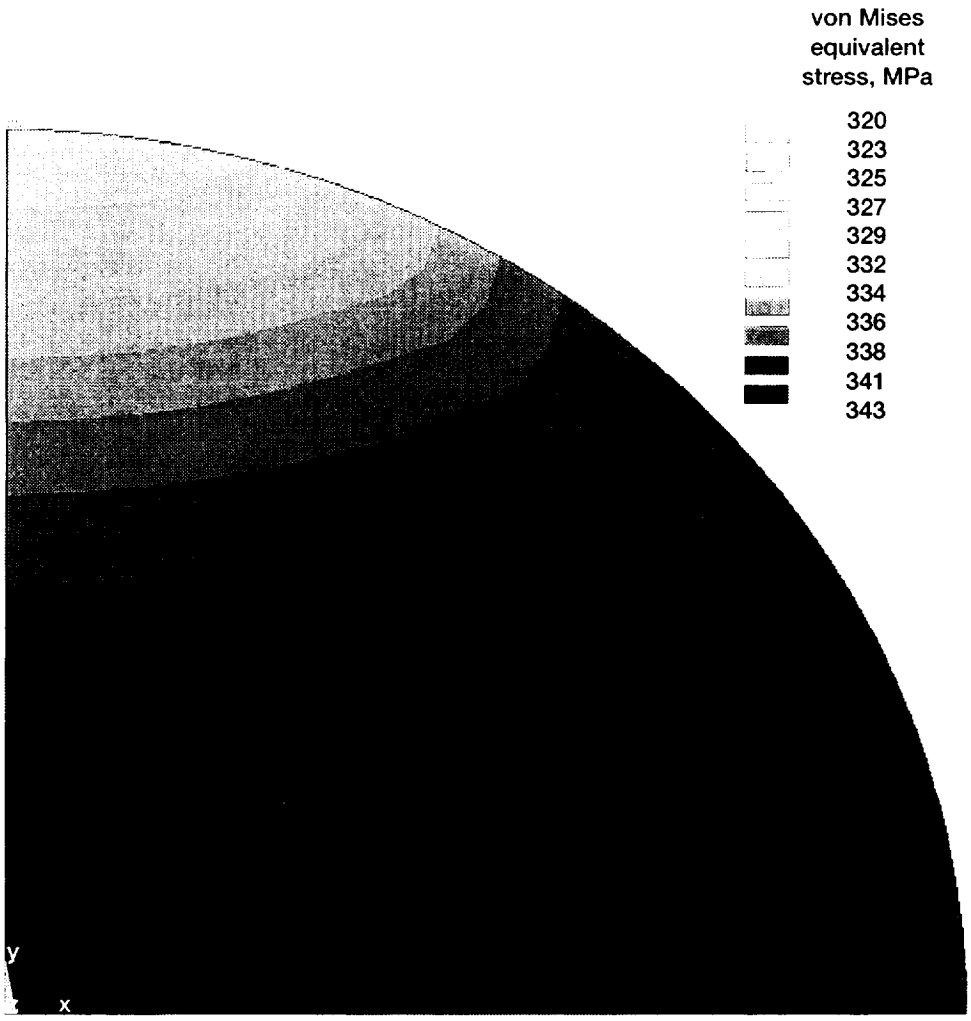

Figure 29.—Stress distribution in specimen gage area: Stress ratio (θ) = −22.5°.

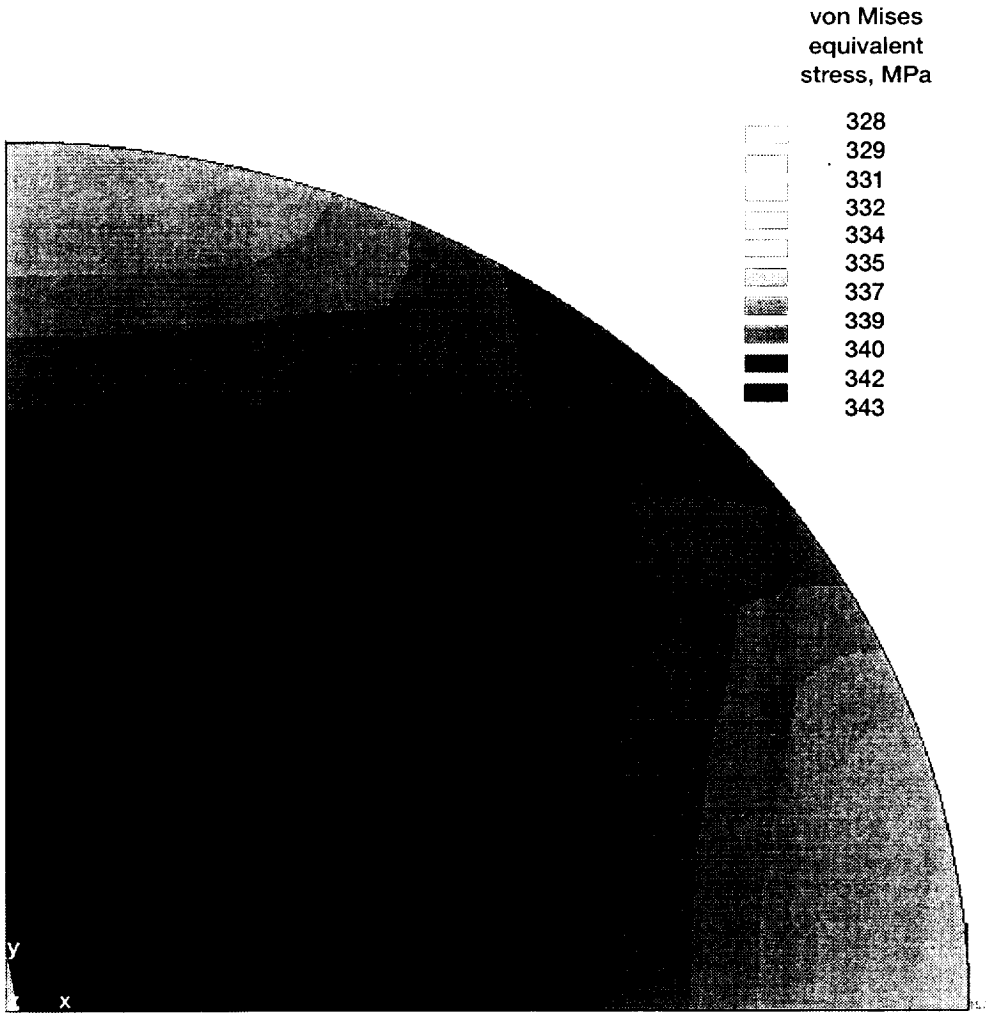

Figure 30.—Stress distribution in specimen gage area: Stress ratio (θ) = –45°.

REPORT DOCUMENTATION PAGE

Form Approved
OMB No. 0704-0188

1. AGENCY USE ONLY (*Leave blank*)	2. REPORT DATE	3. REPORT TYPE AND DATES COVERED
	October 2001	Technical Memorandum

4. TITLE AND SUBTITLE

Specimens and Reusable Fixturing for Testing Advanced Aeropropulsion Materials Under In-Plane Biaxial Loading

Part 1—Results of Conceptual Design Study

5. FUNDING NUMBERS

WU–708–31–13–00

6. AUTHOR(S)

J.R. Ellis, G.S. Sandlass, and M. Bayyari

7. PERFORMING ORGANIZATION NAME(S) AND ADDRESS(ES)

National Aeronautics and Space Administration
John H. Glenn Research Center at Lewis Field
Cleveland, Ohio 44135–3191

8. PERFORMING ORGANIZATION REPORT NUMBER

E–12873

9. SPONSORING/MONITORING AGENCY NAME(S) AND ADDRESS(ES)

National Aeronautics and Space Administration
Washington, DC 20546–0001

10. SPONSORING/MONITORING AGENCY REPORT NUMBER

NASA TM—2001-211134

11. SUPPLEMENTARY NOTES

J.R. Ellis, NASA Glenn Research Center; G.S. Sandlass, MTS Systems Corporation, Eden Prairie, Minnesota 55344; and M. Bayyari, Research Applications, Inc., San Diego, California 92121. Responsible person, J.R. Ellis, organization code 5920, 216–433–3340.

12a. DISTRIBUTION/AVAILABILITY STATEMENT

Unclassified - Unlimited
Subject Category: 24 Distribution: Nonstandard

Available electronically at http://gltrs.grc.nasa.gov/GLTRS

This publication is available from the NASA Center for AeroSpace Information, 301–621–0390.

12b. DISTRIBUTION CODE

13. ABSTRACT ***(Maximum 200 words)***

A design study was undertaken to investigate the feasibility of using simple specimen designs and reusable fixturing for in-plane biaxial tests planned for advanced aeropropulsion materials. Materials of interest in this work include: advanced metallics, polymeric matrix composites, metal and intermetallic matrix composites, and ceramic matrix composites. Early experience with advanced metallics showed that the cruciform specimen design typically used in this type of testing was impractical for these materials, primarily because of concerns regarding complexity and cost. The objective of this research was to develop specimen designs, fixturing, and procedures which would allow in-plane biaxial tests to be conducted on a wide range of aeropropulsion materials while at the same time keeping costs within acceptable limits. With this goal in mind, a conceptual design was developed centered on a specimen incorporating a relatively simple arrangement of slots and fingers for attachment and loading purposes. The ANSYS finite element code was used to demonstrate the feasibility of the approach and also to develop a number of optimized specimen designs. The same computer code was used to develop the reusable fixturing needed to position and grip the specimens in the load frame. The design adopted uses an assembly of slotted fingers which can be reconfigured as necessary to obtain optimum biaxial stress states in the specimen gage area. Most recently, prototype fixturing was manufactured and is being evaluated over a range of uniaxial and biaxial loading conditions.

14. SUBJECT TERMS

In-plane biaxial testing; Advanced aeropropulsion materials; Cruciform specimen design; Reusable fixturing; Finite element analysis; Optimization techniques; Attachment methods; Prototype fixturing

15. NUMBER OF PAGES

52

16. PRICE CODE

17. SECURITY CLASSIFICATION OF REPORT	18. SECURITY CLASSIFICATION OF THIS PAGE	19. SECURITY CLASSIFICATION OF ABSTRACT	20. LIMITATION OF ABSTRACT
Unclassified	Unclassified	Unclassified	